

## Chapter 2

# Phase Formation Rules

Yong Zhang, Sheng Guo, C.T. Liu, and Xiao Yang

**Abstract** This chapter gives an overview of existing active phase formation rules for high-entropy alloys (HEAs). A parametric approach using physiochemical parameters including enthalpy of mixing, entropy of mixing, melting points, atomic size difference, and valence electron concentration is used to delineate phase formation rules for HEAs, with a reference to other multicomponent alloys like bulk metallic glasses (BMGs). Specifically, rules on forming solid solutions, intermetallic compounds, and the amorphous phase are described in detail; formation rules of solid solutions with the face-centered cubic (fcc) or body-centered cubic (bcc) structure are also discussed. Some remaining issues and future prospects on phase formation rules for HEAs are also addressed at the end.

**Keywords** Solid solution • Enthalpy of mixing • Entropy of mixing • Atomic size difference • Electronegativity difference • Valence electron concentration •  $e/a$  ratio • Hume-Rothery rules • Empirical rules • Bulk metallic glasses • Single phase • Face-centered cubic (fcc) • Hexagonal close-packed (hcp) • Body-centered cubic (bcc) • Multiphase • High-entropy alloys (HEAs)

---

Y. Zhang (✉) • X. Yang

State Key Laboratory for Advanced Metals and Materials, University of Science and Technology Beijing, Beijing, People's Republic of China  
e-mail: [drzhangy@ustb.edu.cn](mailto:drzhangy@ustb.edu.cn); [yangxiao\\_sky@163.com](mailto:yangxiao_sky@163.com)

S. Guo

Department of Materials and Manufacturing Technology, Chalmers University of Technology, Gothenburg, SE, Sweden  
e-mail: [sheng.guo@chalmers.se](mailto:sheng.guo@chalmers.se)

C.T. Liu

Department of Mechanical and Biomedical Engineering, City University of Hong Kong, Kowloon Tong, Hong Kong, People's Republic of China  
e-mail: [chainliu@cityu.edu.hk](mailto:chainliu@cityu.edu.hk)

## 2.1 Introduction

The definition of HEAs has been quite controversial. Initially, HEAs were simply defined by their compositional complexity (i.e., composing of at least five major metallic elements, each with a concentration between 5 and 35 at.%) [1]. Recently, this notion has been challenged and the argument is that the microstructural complexity needs to also be considered when classifying HEAs. Particularly, this more strict definition of HEAs requires that the structure of HEAs has to be the single-phased disordered solid solution [2]. Indeed, the much narrower definition of HEAs is more physically justified. From the entropic point of view, the configurational entropies of the multi-principal-element alloys could be low (not really high entropy), if ordered solid solution or intermetallic compounds form. However, new problems also arise with this narrower definition of HEAs. The difficulties include but are not limited to the following situations: in cases where two solid solutions form and also no intermetallic compounds form, which are commonly seen in multi-principal-element alloys [3], can those alloys be classified as HEAs? What is the acceptable threshold configurational entropy (how high is high?) for alloys to be classified as HEAs? If the amorphous phase with a high configurational entropy is formed [4], can those alloys be called HEAs? Practically, it is more convenient to adopt the initial definition of HEAs (i.e., defined from the compositional complexity). [For more information on the history and development of HEAs, please refer to Chap. 1 for details.]

The configurational entropies of compositionally complex alloys are high in the liquid or fully random solid solution state. To avoid further confusions, a sort of arbitrary threshold of configurational entropy larger than  $1.5R$  (where  $R$  is the gas constant) was suggested as an operational definition for HEAs [5]. Then one needs to be aware that different phase constitutions can occur to HEAs, including solid solutions, intermetallic compounds, or even the amorphous phase, depending on the alloy compositions and sometimes the cooling rate if they are prepared by the solidification route [6]. It is within this context that the phase selection among solid solutions, intermetallic compounds, and the amorphous phase in HEAs will be discussed. This will be done using a parametric approach, which utilizes parameters including the atomic size mismatch, mixing enthalpy, the mixing entropy, and melting points [7–10]. These physiochemical parameters [as will be introduced in Sect. 2.2] can reasonably be used to predict the formation of these different phases from the given compositions, although, notably, the occurrence of intermetallic compounds is still difficult to be predicted and controlled. Furthermore, considering the significance of solid solution type on the mechanical properties of HEAs, the phase selection between fcc- and bcc-type solid solutions is discussed in Sect. 2.3, where the electron concentration plays a critical role. Some outstanding issues and future prospects relevant to the phase formation rules for HEAs are addressed in Sect. 2.4, before a summary is given in Sect. 2.5.

## 2.2 Thermodynamics and Geometry Effect

If kinetic factors are not involved, phase formation is thermodynamically controlled by the Gibbs free energy,  $G$ , which is related to the enthalpy,  $H$ , and the entropy,  $S$ , via the following equation, in the case of forming alloys from mixing elemental components:

$$\Delta G_{\text{mix}} = \Delta H_{\text{mix}} - T\Delta S_{\text{mix}} \quad (2.1)$$

Here  $\Delta G_{\text{mix}}$  is the Gibbs free energy of mixing,  $\Delta H_{\text{mix}}$  is the enthalpy of mixing,  $\Delta S_{\text{mix}}$  is the entropy of mixing, and  $T$  is the temperature at which different elements are mixed. Note that the term  $\Delta S_{\text{mix}}$  includes all entropy sources such as configurational, vibrational, electronic, and magnetic contributions. [Please refer to Chaps. 8, 10, and 12 for quantification of the entropy sources in example HEA systems of Co-Cr-Fe-Mn-Ni, Al-Co-Cr-Fe-Ni, and Mo-Nb-Ta-Ti-V-W.] Naturally, it is the competition between  $\Delta H_{\text{mix}}$  and  $T\Delta S_{\text{mix}}$  that determines the phase selection in HEAs. This constitutes the thermodynamic consideration of phase formation rules. Another important effect when considering the phase formation is the geometry effect or, more specifically, the atomic size effect. The atomic size effect is clearly articulated both in the classic Hume-Rothery rules for forming binary solid solutions [11] and the famous Inoue's three empirical rules for the easy formation of BMGs [12]. When establishing phase formation rules for HEAs is addressed using the parametric approach, the descriptors [13] naturally are picked from parameters that are related to the thermodynamics and geometry considerations. Not surprisingly, effective phase formation rules normally comprise both these two considerations.

Figure 2.1 shows a phase selection diagram for multicomponent alloys, including HEAs and BMGs, based on the enthalpy of mixing,  $\Delta H_{\text{mix}}$ , and the atomic size difference, Delta ( $\delta$ ). Here,  $\delta$  is defined as [9]

$$\delta = \sqrt{\sum_{i=1}^N x_i \left(1 - d_i / \sum_{j=1}^N x_j d_j\right)^2} \quad (2.2)$$

where  $N$  is the number of elements,  $x_i$  or  $x_j$  is the composition of the  $i$ th or  $j$ th element, and  $d_i$  or  $d_j$  is the atomic diameter of the  $i$ th or  $j$ th component. The enthalpy of mixing,  $\Delta H_{\text{mix}}$ , for the multicomponent alloys can be estimated by [9]

$$\Delta H_{\text{mix}} = \sum_{i=1, i \neq j}^N 4\Delta H_{\text{AB}}^{\text{mix}} x_i x_j \quad (2.3)$$

where  $\Delta H_{\text{AB}}^{\text{mix}}$  is the enthalpy of mixing for the binary equiatomic AB alloys.

The calculated  $\Delta H_{\text{mix}}$  and  $\delta$  for HEAs and BMGs used in Fig. 2.1 are listed in Table 2.1. It is noted here that the listed phases in Table 2.1 are basically detectable from the X-ray diffraction and they do not necessarily comprise all phases existing in the listed alloys. Seen from Fig. 2.1, in the zone marked **S**, only disordered solid solution will form. In this zone, as the component atomic size difference is

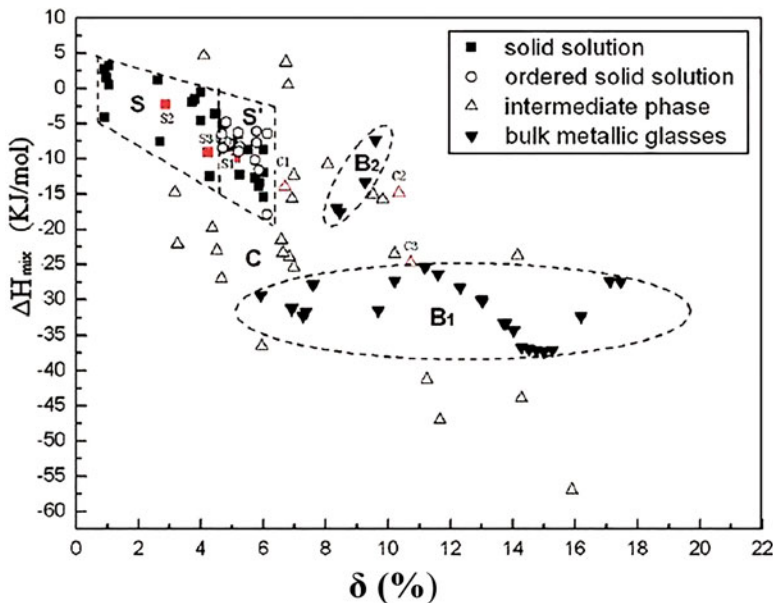


**Fig. 2.1** Phase selection diagram of HEAs and BMGs based on the enthalpy of mixing,  $\Delta H_{\text{mix}}$ , and the atomic size difference, Delta ( $\delta$ ) [9]

relatively small, the component atoms easily substitute for each other and have the similar probability to occupy the lattice sites to form solid solutions. At the same time,  $\Delta H_{\text{mix}}$  is not negative enough for alloys to form a compound. In the zone marked  $S'$ , HEAs still have solid solution as the main phase, but a small amount of the ordered solid solution precipitates in some HEAs. Compared with zone  $S$ ,  $\delta$  increases which deepens the extent of ordering in HEAs.  $\Delta H_{\text{mix}}$  also becomes more negative to promote the precipitation of ordered phases in certain HEAs in zone  $S'$ . BMGs are located in two zones marked **B1** and **B2**. The zone **B2** contains Mg- and Cu-based bulk metallic glasses, while the zone **B1** contains other kinds of BMGs, such as Zr-based bulk metallic glasses. Clearly, compared with HEAs, BMGs have larger  $\delta$  and more negative  $\Delta H_{\text{mix}}$ . Another zone in Fig. 2.1 is marked **C**, in which many intermediate phases will form.

According to Eq. 2.1, at elevated temperatures the high  $\Delta S_{\text{mix}}$  can significantly lower the free energy and thus lower the tendency to order and segregate during the solidification process, which consequently makes solid solution more easily form and more stable than intermetallics or other ordered phases. Therefore, for some HEAs, due to the effect of high  $\Delta S_{\text{mix}}$ , solid solution phases form prior to intermetallics, and the total number of phases is well below the maximum equilibrium number allowed by the Gibbs phase rule. To compare the effect of  $\Delta S_{\text{mix}}$ , Fig. 2.1 is replotted in three dimensions by adding one axis of  $\Delta S_{\text{mix}}$ , as shown in Fig. 2.2. It is apparent that all HEAs have a higher level of  $\Delta S_{\text{mix}}$  than that of BMGs (marked by ▼). The HEAs forming solid solution phases (marked by ■) have  $\Delta S_{\text{mix}}$  in the range of 12–17.5 J/(mol · K) and with smaller values of  $\delta$ . Intermetallic phases (marked by △) form at a

**Table 2.1** Phase constitution; valence electron concentration,  $VEC$ ; enthalpy of mixing,  $\Delta H_{\text{mix}}$ ; entropy of mixing,  $\Delta S_{\text{mix}}$ ; average melting point,  $T_m$ ;  $\Omega$  ( $\Omega = T_m \Delta S_{\text{mix}} / \Delta H_{\text{mix}}$ ); and atomic size difference,  $\delta$ , for representative HEAs and BMGs. Three color codes are used to differentiate solid solutions, solid solutions plus intermetallic compounds, and the amorphous phase forming multicomponent alloys

Alloys	Major phases	$VEC$	$\Delta H_{\text{mix}}$ [kJ/mol]	$\Delta S_{\text{mix}}$ [J/(mol · K)]	$T_m$ (K)	$\Omega$	$\delta$ [%]	Refs.
$\text{Cr}_2\text{CuFe}_2\text{Mn}_2\text{Ni}_2$	fcc	8.11	0.10	13.14	1749.11	229.83	0.91	[10]
$\text{CoCrFeMnNi}$	fcc	8.00	-4.16	13.38	1792.40	5.77	0.92	[10]
$\text{CrCu}_2\text{Fe}_2\text{MnNi}_2$	fcc	8.88	3.88	12.97	1680.88	5.61	0.95	[10]
$\text{CoCrCuFeMnNi}$	fcc	8.50	1.44	14.90	1720.00	17.80	0.99	[10]
$\text{CrCuFeMn}_2\text{Ni}_2$	fcc	8.43	0.44	12.98	1713.00	50.53	0.99	[10]
$\text{CoCrCu}_{0.5}\text{FeNi}$	fcc	8.56	0.49	13.15	1804.67	48.44	1.06	[10]
$\text{CoCrFeNi}$	fcc	8.25	-3.75	11.53	1860.50	5.71	1.06	[10]
$\text{CoCrCuFeNi}$	fcc	8.80	3.20	13.38	1760.00	7.36	1.07	[10]
$\text{CuNi}$	fcc	10.50	4.00	5.76	1543.00	2.22	1.63	[10]
$\text{CoCuFeNiV}$	fcc	8.60	-1.78	14.90	1833.67	15.35	2.63	[10]
$\text{CrCuFeMoNi}$	fcc	8.20	4.64	13.38	1985.00	5.72	2.92	[10]
$\text{CoCrFeMo}_{0.3}\text{Ni}$	fcc	8.09	-4.15	12.83	1932.67	5.97	2.92	[10]
$\text{Al}_{0.25}\text{CrCuFeNi}_2$	fcc	8.71	0.36	12.14	1712.64	57.31	2.93	[16]
$\text{Al}_{0.25}\text{CoCrCu}_{0.75}\text{FeNi}$	fcc	8.40	-0.71	14.32	1738.78	35.07	3.00	[10]
$\text{Al}_{0.3}\text{CoCrCuFeNi}$	fcc	8.47	1.56	14.43	1713.22	15.85	3.15	[10]
$\text{Al}_{0.25}\text{CoCrFeNi}$	fcc	7.94	-6.75	12.71	1805.97	3.40	3.25	[10]
$\text{Al}_{0.3}\text{CoCrFeMo}_{0.1}\text{Ni}$	fcc	7.84	-7.26	13.44	1820.81	3.37	3.74	[10]
$\text{CoCrFeNiPd}$	fcc	8.60	-5.60	13.38	1853.80	4.43	3.76	[20]
$\text{Al}_{0.375}\text{CoCrFeNi}$	fcc	7.80	-7.99	12.97	1781.04	2.89	3.80	[10]
$\text{Al}_{0.5}\text{CoCrCuFeNi}$	fcc	8.27	-1.52	14.70	1684.86	16.29	3.82	[10]
$\text{Al}_{0.5}\text{CrCuFeNi}_2$	fcc	8.45	-2.51	12.60	1677.23	8.41	3.82	[16]
$\text{Al}_{0.5}\text{CoCrCuFeNiV}_{0.2}$	fcc	8.16	-2.50	15.44	1703.01	10.52	3.87	[10]
$\text{Al}_{0.5}\text{CoCrCu}_{0.5}\text{FeNi}$	fcc	8.00	-4.60	14.54	1717.55	5.43	4.00	[10]

(continued)

Table 2.1 (continued)

Alloys	Major phases	VEC	$\Delta H_{\text{mix}}$ [kJ/mol]	$\Delta S_{\text{mix}}$ [J/(mol · K)]	$T_m$ (K)	$\Omega$	$\delta$ [%]	Refs.
$\text{Al}_{0.3}\text{CoCrFeNiTi}_{0.1}$	fcc	7.80	-8.93	13.47	1799.24	2.72	4.06	[10]
$\text{CoCrFeNiPd}_2$	fcc	8.83	-6.11	12.98	1849.33	3.92	4.33	[20]
$\text{CoCrCuFeNiTi}_{0.5}$	fcc	8.36	-3.70	14.70	1776.91	7.05	4.46	[10]
$\text{Co}_{1.5}\text{CrFeNi}_{1.5}\text{Ti}_{0.5}$	fcc	8.09	-10.74	12.86	1848.00	2.22	4.60	[10]
$\text{Co}_{1.5}\text{CrFeNi}_{1.5}\text{Ti}_{0.5}\text{Mo}_{0.1}$	fcc	8.05	-10.64	13.38	1866.70	2.35	4.72	[10]
$\text{Al}_{0.2}\text{Co}_{1.5}\text{CrFeNi}_{1.5}\text{Ti}_{0.5}$	fcc	7.91	-12.50	13.67	1815.91	1.98	5.00	[19]
$\text{Al}_{0.25}\text{CoCrCu}_{0.75}\text{FeNiTi}_{0.5}$	fcc	8.00	-7.28	15.55	1757.61	3.76	5.03	[10]
$\text{Mo}_{25.6}\text{Nb}_{22.7}\text{Ta}_{24.4}\text{W}_{27.3}$	bcc	5.53	-6.49	11.50	3177.60	5.62	2.27	[10]
$\text{Mo}_{21.7}\text{Nb}_{20.6}\text{Ta}_{15.6}\text{V}_{21}\text{W}_{21.1}$	bcc	5.43	-4.54	13.33	2950.49	8.67	3.18	[10]
$\text{Al}_{0.3}\text{CrFe}_{1.5}\text{MnNi}_{0.5}$	bcc	7.19	-5.51	12.31	1747.34	3.90	3.32	[10]
$\text{NbHfTaTiZr}$	bcc	4.40	2.72	13.38	2524.20	12.42	4.01	[21]
$\text{Al}_{0.5}\text{CrFe}_{1.5}\text{MnNi}_{0.5}$	bcc	7.00	-6.77	12.67	1711.17	3.20	4.03	[10]
$\text{AlCrCuFeMnNi}$	bcc	7.50	-5.11	14.90	1580.58	4.62	4.73	[10]
$\text{AlCoCrFeNiSi}_{0.6}$	bcc	6.86	-22.76	14.78	1676.38	1.09	4.98	[22]
$\text{AlCoCrCu}_{0.5}\text{FeNi}$	bcc	7.55	-7.93	14.70	1646.27	3.05	5.02	[10]
$\text{AlCoCrFeNiSi}_{0.4}$	bcc	6.96	-19.84	14.70	1675.98	1.24	5.07	[22]
$\text{AlCoCrCu}_{0.25}\text{FeNi}$	bcc	7.38	-9.94	14.34	1660.00	2.39	5.13	[10]
$\text{AlCoCrFeNiSi}_{0.2}$	bcc	7.08	-16.39	14.22	1675.56	1.45	5.15	[22]
$\text{AlCoCrFeNi}$	bcc	7.20	-12.32	13.38	1675.10	1.83	5.25	[10]
$\text{AlCoCrFeNiMo}_{0.1}$	bcc	7.18	-12.13	13.92	1699.02	1.95	5.30	[23]
$\text{AlCoCrFeNiNb}_{0.1}$	bcc	7.16	-13.32	13.92	1696.18	1.77	5.50	[17]
$\text{Al}_{1.25}\text{CoCrFeNi}$	bcc	7.00	-13.42	13.34	1639.79	1.62	5.55	[10]
$\text{Al}_{2.0}\text{CrCuFeNi}_2$	bcc	7.29	-9.63	12.89	1517.86	2.03	5.71	[16]
$\text{AlCoCrCu}_{0.5}\text{Ni}$	bcc	7.44	-10.17	13.15	1609.67	2.08	5.74	[10]
$\text{Al}_{1.5}\text{CoCrFeNi}$	bcc	6.82	-14.28	13.25	1607.68	1.50	5.77	[10]

$\text{Al}_{2.3}\text{CoCrCuFeNi}$	bcc	6.97	-9.38	14.35	1499.60	2.29	5.84	[10]
$\text{Al}_{2.5}\text{CoCrCuFeNi}$	bcc	6.87	-9.78	14.21	1484.50	2.15	5.91	[10]
$\text{Al}_{2.8}\text{CoCrCuFeNi}$	bcc	6.72	-10.28	14.01	1463.31	1.99	5.99	[10]
$\text{Al}_{20}(\text{CoCrCuFeMnNiVTi})_{80}$	bcc	7.36	-15.44	17.99	1633.50	1.91	6.01	[10]
$\text{Al}_2\text{CoCrFeNi}$	bcc	6.50	-15.44	12.98	1551.50	1.30	6.04	[10]
$\text{Al}_3\text{CoCrCuFeNi}$	bcc	6.63	-10.56	13.86	1450.06	1.90	6.09	[10]
$\text{Al}_{2.5}\text{CoCrFeNi}$	bcc	6.23	-16.09	12.63	1503.96	1.17	6.19	[10]
$\text{Al}_3\text{CoCrFeNi}$	bcc	6.00	-16.41	12.26	1463.21	1.10	6.26	[10]
$\text{AlCoCuNiTiZn}$	bcc	8.17	-17.89	14.90	1680.12	1.39	6.43	[10]
$\text{Al}_{1.5}\text{CoCrFeNiTi}$	bcc	6.38	-20.73	14.78	1659.73	1.18	6.64	[18]
$\text{Al}_2\text{CoCrFeNiTi}$	bcc	6.14	-21.63	14.53	1607.86	1.08	6.64	[18]
$\text{CoCrFeNiTi}_{10.3}$	fcc + hcp	7.95	-8.89	12.83	1866.47	2.69	4.06	[10]
$\text{CrCu}_2\text{Fe}_2\text{Mn}_2\text{Ni}$	bcc + fcc	8.50	4.69	12.97	1654.88	4.58	0.83	[10]
$\text{Cr}_2\text{CuFe}_2\text{MnNi}$	bcc + fcc	8.00	2.61	12.89	1784.86	8.82	0.84	[10]
$\text{CrCuFeMnNi}$	bcc + fcc	8.40	2.72	13.38	1710.00	8.41	0.92	[10]
$\text{Cr}_2\text{Cu}_2\text{Fe}_2\text{MnNi}_2$	bcc + fcc	8.56	3.56	13.14	1729.33	6.38	0.94	[10]
$\text{Cr}_2\text{Cu}_2\text{FeMn}_2\text{Ni}_2$	bcc + fcc	8.44	2.37	13.14	1697.00	9.40	0.97	[10]
$\text{CoCrFeGeMnNi}$	bcc + fcc	7.33	-15.17	14.90	1695.50	1.67	3.25	[10]
$\text{Al}_{0.5}\text{CoCrCuFeNiV}_{0.4}$	bcc + fcc	8.05	-3.34	15.76	1719.92	8.12	3.80	[10]
$\text{Al}_{0.5}\text{CoCrCuFeNiV}_{1.2}$	bcc + fcc	7.69	-5.73	15.98	1777.49	4.96	3.99	[10]
$\text{Al}_{0.5}\text{CoCrCuFeNiV}_2$	bcc + fcc	7.40	-7.08	15.60	1822.77	4.01	3.99	[10]
$\text{Al}_{0.5}\text{CoCrCuFeNiV}_{1.4}$	bcc + fcc	7.61	-6.14	15.91	1789.79	4.64	4.00	[10]
$\text{Al}_{0.5}\text{CoCrCuFeNiV}_{1.6}$	bcc + fcc	7.54	-6.50	15.82	1801.40	4.38	4.00	[10]
$\text{Al}_{0.5}\text{CoCrCuFeNiV}_{1.8}$	bcc + fcc	7.47	-6.81	15.72	1812.38	4.19	4.00	[10]
$\text{Al}_{0.5}\text{CoCrFeNi}$	bcc + fcc	7.67	-9.09	13.15	1757.50	2.55	4.22	[10]
$\text{Al}_{0.8}\text{CoCrCuFeNi}$	bcc + fcc	8.00	-3.61	14.87	1646.00	6.78	4.49	[10]
$\text{AlCoCrCuFeNiSi}$	bcc + fcc	7.29	-18.86	16.18	1631.50	1.40	4.51	[10]

(continued)

**Table 2.1** (continued)

Alloys	Major phases	VEC	$\Delta H_{\text{mix}}$ [kJ/mol]	$\Delta S_{\text{mix}}$ [J/(mol · K)]	$T_m$ (K)	$\Omega$	$\delta$ [%]	Refs.
AlCoCrCuFeNiV	bcc + fcc	7.43	-7.76	16.18	1705.07	3.56	4.69	[10]
Al <sub>0.75</sub> CoCrCu <sub>0.25</sub> FeNi	bcc + fcc	7.60	-8.47	14.32	1696.33	2.87	4.71	[10]
AlCrCuFeNi <sub>2</sub>	bcc + fcc	8.00	-5.78	12.98	1615.25	3.63	4.82	[16]
AlCoCrCuFeNi	bcc + fcc	7.83	-4.78	14.90	1622.25	5.06	4.82	[10]
Al <sub>0.5</sub> CoCrFeNi	bcc + fcc	7.42	-10.90	13.33	1714.13	2.09	4.83	[10]
AlCo <sub>0.5</sub> CrCuFeNi	bcc + fcc	7.73	-4.50	14.70	1608.82	5.26	4.91	[10]
AlCoCrCuFeNi <sub>0.5</sub>	bcc + fcc	7.64	-3.90	14.70	1612.64	6.08	4.91	[10]
AlCoCrCuFeMo <sub>0.2</sub> Ni	bcc + fcc	7.77	-4.47	15.60	1633.31	5.70	4.95	[10]
AlCoCrCuFe <sub>0.5</sub> Ni	bcc + fcc	7.82	-5.55	14.70	1605.09	4.25	5.00	[10]
AlCoCr <sub>0.5</sub> CuFeNi	bcc + fcc	8.00	-5.02	14.70	1572.82	4.61	5.02	[10]
Al <sub>0.875</sub> CoCrFeNi	bcc + fcc	7.31	-11.66	13.37	1694.12	1.95	5.06	[10]
Al <sub>1.3</sub> CoCrCuFeNi	bcc + fcc	7.60	-6.24	14.85	1589.45	3.78	5.19	[10]
AlCoCrCuNi	bcc + fcc	7.80	-6.56	13.38	1584.50	3.23	5.19	[10]
Al <sub>0.5</sub> CoCeCu <sub>0.5</sub> FeNiTi <sub>0.5</sub>	bcc + fcc	7.09	-10.84	15.75	1738.32	2.52	5.25	[10]
Al <sub>1.5</sub> CrCuFeNi <sub>2</sub>	bcc + fcc	7.62	-8.05	13.01	1562.81	2.53	5.38	[16]
Al <sub>1.5</sub> CoCrCuFeNi	bcc + fcc	7.46	-7.04	14.78	1569.27	3.30	5.38	[10]
Al <sub>1.8</sub> CoCrCuFeNi	bcc + fcc	7.26	-8.08	14.65	1541.22	2.79	5.54	[10]
AlCo <sub>3</sub> CrFeNiTi <sub>0.5</sub>	bcc + fcc	7.47	-14.93	13.49	1718.47	1.55	5.69	[10]
Al <sub>2</sub> CoCrCuFeNi	bcc + fcc	7.14	-8.65	14.53	1523.86	2.56	5.71	[10]
AlCr <sub>3</sub> CuFeNiTi	bcc + fcc	6.75	-9.31	13.86	1794.44	2.67	5.72	[10]
Al <sub>11.1</sub> (CoCrCuFeMnNiV <sub>1</sub> Ti) <sub>88.9</sub>	bcc + fcc	7.43	-12.74	18.27	1711.28	2.45	5.75	[10]
AlCoCuNi	bcc + fcc	8.25	-8.00	11.52	1447.40	2.08	5.77	[10]
AlCoCrCuFeNiTiV	bcc + fcc	7.00	-13.94	17.29	1735.19	2.15	5.87	[10]
AlCo <sub>2</sub> CrFeNiTi <sub>0.5</sub>	bcc + fcc	7.23	-16.43	14.23	1710.54	1.49	5.91	[10]
AlCr <sub>2</sub> CuFeNiTi	bcc + fcc	6.86	-11.10	14.53	1746.07	2.29	5.99	[10]

AlCo <sub>1.5</sub> CrFeNiTi <sub>0.5</sub>	bcc + fcc	7.08	-17.17	14.54	1705.58	1.45	6.02	[10]
AlCr <sub>1.5</sub> CuFeNiTi	bcc + fcc	6.92	-12.26	14.78	1716.31	2.08	6.14	[10]
AlCuNi	bcc + fcc	8.00	-8.44	9.13	1339.80	1.45	6.20	[10]
AlCrCuFeNiTi	bcc + fcc	7.00	-13.67	14.90	1681.58	1.83	6.29	[10]
AlCr <sub>0.5</sub> CuFeNiTi	bcc + fcc	7.09	-15.40	14.70	1640.55	1.56	6.45	[10]
Al <sub>0.75</sub> CoCrCu <sub>0.25</sub> FeNiTi <sub>0.5</sub>	bcc1 + bcc2	7.00	-15.26	15.55	1719.02	1.75	5.83	[10]
AlCoCrCu <sub>0.5</sub> FeNiTi <sub>0.5</sub>	bcc1 + bcc2	7.25	-13.42	15.86	1671.25	1.97	5.90	[10]
AlCoCrCu <sub>0.25</sub> FeNiTi <sub>0.5</sub>	bcc1 + bcc2	7.09	-15.50	15.54	1684.87	1.68	6.01	[10]
AlCoCrFeNiTi <sub>0.5</sub>	bcc1 + bcc2	6.91	-17.92	14.70	1699.73	1.39	6.11	[10]
AlCoCrCuFeNiTi	bcc1 + bcc2 + fcc	7.29	-13.80	16.18	1668.50	1.95	6.23	[10]
AlCoCrFeNiTi	bcc1 + bcc2	6.67	-21.56	14.90	1720.25	1.19	6.58	[10]
Al <sub>0.5</sub> CoCrCuFeNiV <sub>0.6</sub>	bcc + fcc + $\sigma$ -phase	7.95	-4.07	15.92	1735.73	6.79	3.94	[10]
Al <sub>0.5</sub> CoCrCuFeNiV <sub>0.8</sub>	bcc + fcc + $\sigma$ -phase	7.86	-4.71	16.00	1750.53	5.95	3.97	[10]
Al <sub>0.5</sub> CoCrCuFeNiV	bcc + fcc + $\sigma$ -phase	7.77	-5.25	16.01	1764.42	5.38	3.98	[10]
AlCoCrCuFeMnNi	bcc + fcc + unknown phase	7.71	-5.63	16.18	1607.64	4.61	4.57	[10]
AlCoCrCuFeMnNi	bcc + fcc + unknown phase	7.71	-5.63	16.18	1607.64	4.61	4.57	[10]
AlCoCrFeNiSi	bcc + $\delta$ -phase	6.67	-27.33	14.90	1677.08	0.91	4.82	[22]
AlCoCrFeNiSi <sub>0.8</sub>	bcc + $\delta$ -phase	6.76	-25.23	14.87	1676.74	0.99	4.90	[22]
AlCrMoSiTi	Ordered bcc + Mo <sub>5</sub> Si <sub>3</sub>	4.60	-34.08	13.38	1918.90	0.75	4.91	[10]
AlCoCrCuFeNiMo <sub>0.4</sub>	bcc + $\alpha$ -phase	7.72	-4.20	15.91	1701.80	6.45	5.05	[10]
Co <sub>1.5</sub> CrFeMo <sub>0.5</sub> Ni <sub>1.5</sub> Ti <sub>0.5</sub>	fcc + $\sigma$ -phase	7.92	-10.25	14.17	1935.25	2.67	5.09	[10]
AlCoCr <sub>2</sub> FeMo <sub>0.5</sub> Ni	bcc + $\sigma$	6.92	-10.27	14.23	1839.38	2.55	5.10	[24]
AlCoCrCuFeNiMo <sub>0.6</sub>	bcc + $\alpha$ -phase	7.67	-3.95	16.08	1737.95	7.07	5.13	[10]
AlCoCrFe <sub>2</sub> Mo <sub>0.5</sub> Ni	bcc + $\alpha$ -phase	7.23	-9.70	14.23	1789.85	2.63	5.15	[10]
CoCrCuFeMnNiTiV	fcc + bcc + $\sigma$ -phase + unknown phase	7.50	-8.13	17.29	1808.50	3.85	5.19	[10]
AlCoCrCuFeNiMo <sub>0.8</sub>	bcc + $\alpha$ -phase	7.62	-3.72	16.16	1771.99	7.69	5.20	[10]

(continued)

Table 2.1 (continued)

Alloys	Major phases	VEC	$\Delta H_{\text{mix}}$ [kJ/mol]	$\Delta S_{\text{mix}}$ [J/(mol · K)]	$T_m$ (K)	$\Omega$	$\delta$ [%]	Refs.
AlCoCrCuFeNiMo	bcc + $\alpha$ -phase	7.57	-3.51	16.18	1804.07	8.32	5.25	[10]
CoCrCuFeNiTi <sub>0.8</sub>	fcc + Laves phase	8.14	-6.75	14.89	1785.66	3.95	5.26	[10]
AlCoCr <sub>1.5</sub> FeMo <sub>0.5</sub> Ni	bcc + $\sigma$	7.00	-10.83	14.53	1814.92	2.43	5.27	[24]
Co <sub>1.5</sub> CrFeMo <sub>0.8</sub> Ni <sub>1.5</sub> Ti <sub>0.5</sub>	fcc + $\sigma$ -phase	7.83	-9.96	14.21	1980.95	2.83	5.28	[10]
AlCo <sub>2</sub> CrFeMo <sub>0.5</sub> Ni	bcc + fcc + $\sigma$ -phase	7.38	-10.70	14.23	1783.54	2.37	5.29	[10]
AlCoCrFe <sub>1.5</sub> Mo <sub>0.5</sub> Ni	bcc + $\sigma$ -phase	7.17	-10.50	14.53	1788.08	2.47	5.30	[10]
AlCoCrFeMo <sub>0.5</sub> Ni	bcc + $\alpha$ -phase	7.15	-11.95	14.22	1722.02	2.05	5.35	[23]
AlCo <sub>1.5</sub> CrFeMo <sub>0.5</sub> Ni	bcc + $\sigma$ -phase	7.25	-11.08	14.53	1784.67	2.34	5.39	[10]
AlCoCrFeMo <sub>0.3</sub> Ni	bcc + $\alpha$ -phase	7.13	-11.78	14.43	1744.15	2.14	5.40	[23]
AlCoCrFeMo <sub>0.4</sub> Ni	bcc + $\alpha$ -phase	7.11	-11.60	14.59	1765.46	2.22	5.44	[23]
AlCoCrFeMo <sub>0.5</sub> Ni	bcc + $\sigma$ -phase	7.09	-11.44	14.70	1786.00	2.29	5.47	[10]
AlCoCrFeMo <sub>0.5</sub> Ni	bcc + $\sigma$	7.09	-11.44	14.70	1786.00	2.29	5.47	[24]
AlCoCrFeMo <sub>0.5</sub> Ni	bcc + $\alpha$ -phase	7.09	-11.44	14.70	1786.00	2.29	5.47	[23]
AlCo <sub>0.5</sub> CrFeMo <sub>0.5</sub> Ni	bcc + $\sigma$ -phase	6.90	-11.72	14.53	1787.60	2.22	5.54	[10]
AlCoCrFe <sub>0.6</sub> Mo <sub>0.5</sub> Ni	bcc + $\sigma$ -phase	7.02	-12.32	14.61	1784.04	2.12	5.61	[10]
CoCrCuFeNiTi	fcc + Laves phase	8.00	-8.44	14.90	1791.00	3.17	5.65	[10]
AlCoCr <sub>0.5</sub> FeMo <sub>0.5</sub> Ni	bcc + $\sigma$	7.20	-12.08	14.53	1750.06	2.11	5.69	[24]
Al <sub>0.5</sub> B <sub>0.2</sub> CoCrCuFeNi	fcc + boride	8.09	-4.00	15.44	1708.73	6.60	5.77	[10]
AlCoCrFeNb <sub>0.25</sub> Ni	bcc + Laves phase	7.10	-14.66	14.34	1726.29	1.69	5.83	[17]
Co <sub>1.5</sub> CrFeNi <sub>1.5</sub> Ti	fcc + $\eta$	7.75	-15.61	13.21	1856.17	1.57	5.83	[19]
AlCoFeMo <sub>0.5</sub> Ni	bcc + $\sigma$	7.33	-12.74	13.15	1708.89	1.76	5.93	[24]
Al <sub>0.2</sub> Co <sub>1.5</sub> CrFeNi <sub>1.5</sub> Ti	fcc + $\eta$	7.60	-17.12	13.97	1826.40	1.49	6.01	[19]
Al <sub>3.0</sub> CrCuFeNi <sub>2</sub>	bcc + ordered bcc	6.75	-11.50	12.42	1444.81	1.56	6.03	[16]
Al <sub>40</sub> (CoCrCuFeMnNiTiV) <sub>60</sub>	bcc + Al <sub>3</sub> Ti + unknown phase	5.70	-18.29	15.97	1458.50	1.27	6.09	[10]
CoCrFeNiTi	fcc + bcc + CoTi <sub>2</sub>	7.40	-16.32	13.38	1877.60	1.54	6.13	[18]

AlAuCoCrCuNi	fcc + AuCu	8.33	-6.45	14.90	1543.42	3.57	6.14	[10]
AlCoCrFeNb <sub>0.5</sub> Ni	bcc + Laves phase	7.00	-16.53	14.70	1772.82	1.58	6.24	[17]
Al <sub>0.5</sub> CoCrFeNiTi	fcc + bcc + CoTi <sub>2</sub> + FeTi	7.00	-16.79	14.70	1791.77	1.57	6.44	[18]
AlCoCrFeNb <sub>0.75</sub> Ni	bcc + Laves phase	6.91	-18.03	14.85	1815.30	1.50	6.55	[17]
AlCoCrFeNiTi	fcc + bcc + CoTi <sub>2</sub> + FeTi	6.67	-19.22	14.90	1720.25	1.33	6.58	[18]
AlCoCrFeNiTi <sub>1.5</sub>	bcc1 + bcc2 + Laves phase	6.46	-23.91	14.78	1737.62	1.08	6.93	[10]
Al <sub>0.5</sub> B <sub>0.6</sub> CoCrCuFeNi	fcc + boride	7.75	-8.01	15.92	1751.76	3.48	8.07	[10]
Al <sub>0.5</sub> BCoCrCuFeNi	fcc + ordered fcc + boride	7.46	-11.03	16.01	1789.50	2.60	9.52	[10]
CrCuFeNiZr	bcc + compounds	7.80	-14.40	13.38	1831.60	1.70	9.91	[10]
CoCrCuFeNiTi <sub>2</sub>	Compounds	7.43	-14.04	14.53	1813.14	1.87	6.69	[10]
AlCoCrCuNiTiY <sub>0.5</sub>	Cu <sub>2</sub> Y + AlNi <sub>2</sub> Ti + Cu + Cr	6.85	-18.32	16.00	1935.38	1.68	7.53	[10]
CuFeHfTiZr	Compounds	6.20	-15.84	13.38	1949.40	1.64	9.84	[10]
CoCuHfTiZr	Compounds	6.40	-23.52	13.38	1941.20	1.11	10.21	[10]
AlTiVYZr	Compounds	3.80	-14.88	13.38	1802.10	1.62	10.35	[10]
BeCuNiTiVZr	Compounds	6.00	-24.89	14.90	1820.67	1.09	11.09	[10]
AlCoCrCuNiTiY <sub>0.8</sub>	Cu <sub>2</sub> Y + AlNi <sub>2</sub> Ti + Cu + Cr	6.68	-19.00	16.16	1929.45	1.64	12.73	[10]
AlCoCrCuNiTiY	Cu <sub>2</sub> Y + AlNi <sub>2</sub> Ti + Cu + Cr + unknown phase	6.57	-19.37	16.18	1925.79	1.62	13.45	[10]
Cu <sub>47</sub> Ti <sub>33</sub> Zr <sub>11</sub> Si <sub>1</sub> Ni <sub>6</sub> Sn <sub>2</sub>	Amorphous	7.65	-17.02	10.45	1645.17	1.01	8.36	[10]
Cu <sub>47</sub> Ti <sub>33</sub> Zr <sub>11</sub> Si <sub>1</sub> Ni <sub>8</sub>	Amorphous	7.77	-17.56	10.07	1669.63	0.96	8.46	[10]
Ti <sub>45</sub> Cu <sub>25</sub> Ni <sub>15</sub> Sn <sub>3</sub> Be <sub>7</sub> Zr <sub>5</sub>	Amorphous	6.51	-21.22	11.90	1705.29	0.96	9.08	[10]
Mg <sub>65</sub> Cu <sub>15</sub> Ag <sub>5</sub> Pd <sub>5</sub> Y <sub>10</sub>	Amorphous	4.30	-13.24	9.10	1074.86	0.74	9.27	[10]
Mg <sub>65</sub> Cu <sub>15</sub> Ag <sub>5</sub> Pd <sub>5</sub> Gd <sub>10</sub>	Amorphous	4.30	-13.24	9.10	1053.49	0.72	9.27	[10]
Mg <sub>65</sub> Cu <sub>7.5</sub> Ni <sub>7.5</sub> Zn <sub>5</sub> Ag <sub>5</sub> Y <sub>10</sub>	Amorphous	4.33	-7.35	9.96	1107.24	1.50	9.53	[10]
Zr <sub>57</sub> Ti <sub>5</sub> Al <sub>10</sub> Cu <sub>20</sub> Ni <sub>8</sub>	Amorphous	5.78	-31.50	10.18	1813.45	0.59	9.69	[10]
Co <sub>64.8</sub> Fe <sub>7.2</sub> B <sub>19.2</sub> Si <sub>4.8</sub> Nb <sub>4</sub>	Amorphous	7.38	-24.16	8.83	1922.41	0.70	10.02	[30]
Co <sub>57.8</sub> Fe <sub>14.4</sub> B <sub>19.2</sub> Si <sub>4.8</sub> Nb <sub>4</sub>	Amorphous	7.30	-24.27	9.88	1925.36	0.78	10.05	[30]

(continued)

**Table 2.1** (continued)

Alloys	Major phases	VEC	$\Delta H_{\text{mix}}$ [kJ/mol]	$\Delta S_{\text{mix}}$ [J/(mol · K)]	$T_m$ (K)	$\Omega$	$\delta$ [%]	Refs.
$\text{Co}_{50.4}\text{Fe}_{21.6}\text{B}_{19.2}\text{Si}_{4.8}\text{Nb}_4$	Amorphous	7.23	-24.34	10.54	1928.31	0.83	10.08	[30]
$\text{Co}_{43.2}\text{Fe}_{28.8}\text{B}_{19.2}\text{Si}_{4.8}\text{Nb}_4$	Amorphous	7.16	-24.37	10.91	1931.26	0.86	10.12	[30]
$\text{CuNiHfTiZr}$	Amorphous	6.60	-27.36	13.38	1932.80	0.95	10.21	[10]
$\text{Ni}_{45}\text{Ti}_{20}\text{Zr}_{25}\text{Al}_{10}$	Amorphous	6.60	-45.41	10.46	1792.15	0.41	10.35	[27]
$\text{Ni}_{40}\text{Cu}_5\text{Ti}_{17}\text{Zr}_{28}\text{Al}_{10}$	Amorphous	6.65	-43.25	11.67	1779.11	0.48	10.48	[27]
$\text{Ni}_{39.8}\text{Cu}_{5.97}\text{Ti}_{15.92}\text{Zr}_{27.86}\text{Al}_{6.95}\text{Si}_{0.5}$	Amorphous	6.71	-43.58	11.97	1772.80	0.49	10.50	[27]
$\text{Ni}_{40}\text{Cu}_6\text{Ti}_{16}\text{Zr}_{28}\text{Al}_{10}$	Amorphous	6.72	-42.79	11.77	1773.23	0.49	10.52	[27]
$\text{Ti}_{55}\text{Zr}_{10}\text{Cu}_{60}\text{Ni}_8\text{Be}_{18}$	Amorphous	4.75	-25.43	10.70	1824.72	0.77	11.18	[10]
$\text{Ti}_{50}\text{Zr}_{15}\text{Cu}_{60}\text{Ni}_8\text{Be}_{18}$	Amorphous	4.75	-26.37	11.30	1833.82	0.79	11.64	[10]
$\text{Ti}_{40}\text{Zr}_{25}\text{Ni}_{13}\text{Cu}_{12}\text{Be}_{20}$	Amorphous	4.62	-25.88	11.60	2010.40	0.90	12.03	[10]
$\text{Ni}_{40}\text{Cu}_5\text{Ti}_{16.5}\text{Zr}_{28.5}\text{Al}_{10}$	Amorphous	6.65	-43.41	11.65	1780.02	0.48	12.07	[27]
$\text{Ti}_{40}\text{Zr}_{25}\text{Cu}_{60}\text{Ni}_8\text{Be}_{18}$	Amorphous	4.75	-28.26	11.98	1852.02	0.79	12.31	[10]
$\text{Mg}_{65}\text{Cu}_{20}\text{Zn}_5\text{Y}_{10}$	Amorphous	4.40	-5.98	8.16	1085.64	1.48	12.70	[10]
$\text{Fe}_{61}\text{B}_{15}\text{Mo}_7\text{Zr}_8\text{Co}_7\text{Y}_2$	Amorphous	6.76	-30.13	10.30	1992.27	0.68	13.20	[10]
$\text{Fe}_{61}\text{B}_{15}\text{Mo}_7\text{Zr}_8\text{Co}_5\text{Y}_2\text{Cr}_2$	Amorphous	6.70	-29.97	10.65	1999.53	0.71	13.20	[10]
$\text{Fe}_{61}\text{B}_{15}\text{Mo}_7\text{Zr}_8\text{Co}_6\text{Y}_2\text{Al}_1$	Amorphous	6.70	-30.30	10.54	1983.91	0.69	13.24	[10]
$\text{Zr}_{38.5}\text{Ti}_{16.5}\text{Cu}_{15.25}\text{Ni}_{9.75}\text{Be}_{20}$	Amorphous	5.25	-33.20	12.47	1828.35	0.69	13.36	[10]
$\text{Zr}_{39.88}\text{Ti}_{15.12}\text{Cu}_{13.77}\text{Ni}_{9.98}\text{Be}_{21.25}$	Amorphous	5.14	-34.27	12.34	1834.26	0.66	13.59	[10]
$\text{Er}_{20}\text{Tb}_{20}\text{Dy}_{20}\text{Ni}_{20}\text{Al}_{20}$	Amorphous	4.40	-37.60	13.38	1554.90	0.55	13.66	[25]
$\text{Dy}_{46}\text{Al}_{24}\text{Co}_{18}\text{Fe}_2\text{Y}_{10}$	Amorphous	4.18	-33.26	10.95	1533.60	0.50	13.71	[10]
$\text{Co}_{45.5}\text{Fe}_{2.5}\text{Cr}_{15}\text{Mo}_{14}\text{C}_{15}\text{B}_6\text{Er}_2$	Amorphous	6.88	-33.41	12.82	2327.43	0.89	13.79	[31]
$\text{Co}_{43}\text{Fe}_3\text{Cr}_{13}\text{Mo}_{14}\text{C}_{15}\text{B}_6\text{Er}_2$	Amorphous	6.85	-33.46	13.34	2369.44	0.94	13.80	[31]
$\text{Zr}_{41.2}\text{Ti}_{13.8}\text{Cu}_{12.5}\text{Ni}_{10}\text{Be}_{22.5}$	Amorphous	5.03	-36.72	12.18	1839.28	0.61	13.82	[10]
$\text{Zr}_{42.63}\text{Ti}_{12.37}\text{Cu}_{11.25}\text{Ni}_{10}\text{Be}_{23.75}$	Amorphous	4.91	-36.90	11.97	1844.44	0.60	14.05	[10]
$\text{Ce}_{65}\text{Al}_{10}\text{Ni}_{10}\text{Cu}_{10}\text{Nb}_5$	Amorphous	4.60	-19.86	9.32	1236.25	0.58	14.18	[26]

Zr <sub>44</sub> Ti <sub>11</sub> Cu <sub>10</sub> Ni <sub>10</sub> Be <sub>25</sub>	Amorphous	4.80	-37.07	11.73	1849.48	0.59	14.27	[10]
Zr <sub>45.38</sub> Ti <sub>9.62</sub> Cu <sub>8.75</sub> Ni <sub>10</sub> Be <sub>26.25</sub>	Amorphous	4.69	-37.23	11.46	1845.09	0.57	14.49	[10]
Gd <sub>36</sub> Y <sub>20</sub> Al <sub>24</sub> Co <sub>20</sub>	Amorphous	4.20	-34.26	11.26	1509.56	0.50	14.49	[32]
Zr <sub>46.75</sub> Ti <sub>8.25</sub> Cu <sub>7.5</sub> Ni <sub>10</sub> Be <sub>27.5</sub>	Amorphous	4.58	-37.03	11.16	1848.95	0.56	14.70	[10]
La <sub>68</sub> Al <sub>14</sub> (Cu <sub>5/6</sub> Ag <sub>1/6</sub> ) <sub>8</sub> Ni <sub>5</sub> Co <sub>5</sub>	Amorphous	4.29	-26.33	8.94	1224.51	0.42	14.93	[29]
La <sub>32</sub> Ce <sub>32</sub> Al <sub>16</sub> Ni <sub>5</sub> Cu <sub>12</sub> Co <sub>3</sub>	Amorphous	4.49	-27.96	12.74	1221.42	0.56	15.05	[33]
La <sub>32</sub> Ce <sub>32</sub> Al <sub>16</sub> Ni <sub>5</sub> Cu <sub>10</sub> Co <sub>5</sub>	Amorphous	4.45	-25.71	12.11	1229.66	0.62	15.11	[33]
Sr <sub>20</sub> Ca <sub>20</sub> Yb <sub>20</sub> Mg <sub>20</sub> Zn <sub>20</sub>	Amorphous	4.20	-13.12	13.38	973.54	0.99	15.25	[25]
Ce <sub>60</sub> Al <sub>15</sub> Ni <sub>15</sub> Cu <sub>10</sub>	Amorphous	4.85	-30.60	9.19	1178.23	0.35	15.29	[26]
La <sub>66</sub> Al <sub>14</sub> (Cu <sub>5/6</sub> Ag <sub>1/6</sub> ) <sub>10</sub> Ni <sub>5</sub> Co <sub>5</sub>	Amorphous	4.45	-26.73	9.35	1227.38	0.43	15.32	[29]
La <sub>32</sub> Ce <sub>32</sub> Al <sub>16</sub> Ni <sub>5</sub> Cu <sub>3</sub> Co <sub>12</sub>	Amorphous	4.31	-27.92	12.74	1258.50	0.57	15.33	[33]
Sr <sub>20</sub> Ca <sub>20</sub> Yb <sub>20</sub> (Li <sub>0.55</sub> Mg <sub>0.45</sub> ) <sub>20</sub> Zn <sub>20</sub>	Amorphous	4.09	-12.15	14.53	922.03	1.10	15.49	[25]
La <sub>62</sub> Al <sub>14</sub> Cu <sub>20</sub> Ag <sub>4</sub>	Amorphous	4.92	-26.72	8.50	1191.97	0.38	15.49	[28]
La <sub>65</sub> Al <sub>14</sub> (Cu <sub>5/6</sub> Ag <sub>1/6</sub> ) <sub>11</sub> Ni <sub>5</sub> Co <sub>5</sub>	Amorphous	4.53	-26.86	9.54	1228.82	0.44	15.51	[29]
Ce <sub>57</sub> Al <sub>10</sub> Ni <sub>12.5</sub> Cu <sub>15.5</sub> Nb <sub>5</sub>	Amorphous	5.22	-22.06	10.39	1268.38	0.60	15.53	[26]
La <sub>64</sub> Al <sub>14</sub> (Cu <sub>5/6</sub> Ag <sub>1/6</sub> ) <sub>12</sub> Ni <sub>5</sub> Co <sub>5</sub>	Amorphous	4.61	-27.06	9.72	1230.25	0.44	15.68	[29]
La <sub>62</sub> Al <sub>14</sub> (Cu <sub>5/6</sub> Ag <sub>1/6</sub> ) <sub>20</sub> Ni <sub>5</sub> Co <sub>2</sub>	Amorphous	4.86	-26.89	9.48	1208.43	0.43	15.70	[28]
Nd <sub>60</sub> Al <sub>10</sub> Ni <sub>10</sub> Cu <sub>20</sub>	Amorphous	5.30	-27.48	9.05	1311.75	0.43	15.70	[32]
La <sub>32</sub> Ce <sub>32</sub> Al <sub>16</sub> Ni <sub>5</sub> Cu <sub>15</sub>	Amorphous	4.55	-23.80	12.11	1209.06	0.62	15.72	[33]
Pr <sub>60</sub> Al <sub>10</sub> Ni <sub>10</sub> Cu <sub>20</sub>	Amorphous	5.30	-27.52	9.05	1260.75	0.41	15.94	[32]
La <sub>62</sub> Al <sub>14</sub> (Cu <sub>5/6</sub> Ag <sub>1/6</sub> ) <sub>14</sub> Ni <sub>5</sub> Co <sub>5</sub>	Amorphous	4.77	-27.31	10.06	1233.12	0.45	16.02	[28]
La <sub>35</sub> Al <sub>25</sub> Ni <sub>5</sub> Cu <sub>10</sub> Co <sub>5</sub>	Amorphous	4.45	-32.31	10.02	1200.78	0.37	16.19	[10]
Sr <sub>20</sub> Ca <sub>20</sub> Yb <sub>20</sub> Mg <sub>20</sub> Zn <sub>10</sub> Cu <sub>10</sub>	Amorphous	3.70	-10.60	14.53	1040.07	1.43	16.35	[25]
(CeLaPrPd) <sub>65</sub> Co <sub>25</sub> Al <sub>10</sub>	Amorphous	5.64	-47.60	14.62	1396.78	0.43	16.78	[34]
Nd <sub>60</sub> Al <sub>15</sub> Ni <sub>10</sub> Cu <sub>10</sub> Fe <sub>5</sub>	Amorphous	5.95	-27.37	9.99	1313.18	0.48	17.11	[10]
Nd <sub>61</sub> Al <sub>11</sub> Ni <sub>8</sub> Co <sub>5</sub> Cu <sub>15</sub>	Amorphous	6.28	-27.43	9.82	1307.13	0.47	17.46	[10]

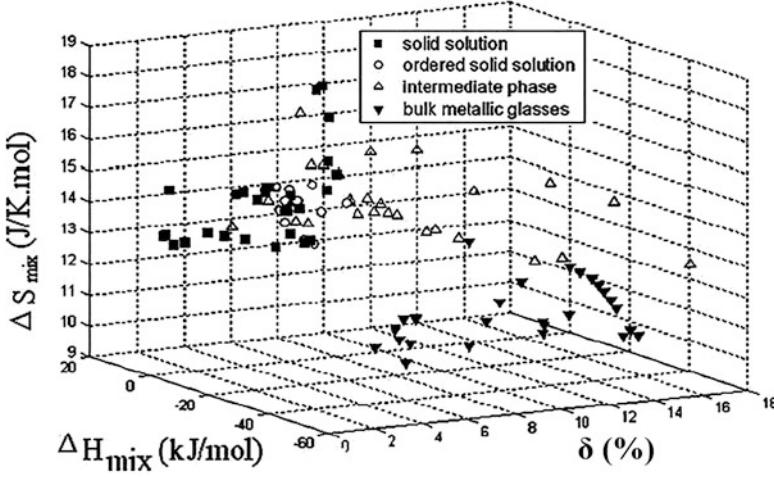


Fig. 2.2 Phase selection diagram of HEAs and BMGs based on  $\Delta H_{\text{mix}}$ ,  $\Delta S_{\text{mix}}$ , and  $\delta$  [9]

larger value of  $\delta$ , but with the  $\Delta S_{\text{mix}}$  in the range of 11–16.5 J/(mol·K). There is a transition zone (marked by  $\circ$ ) between the solid solution phase zone and the intermetallic compound zone, which contains ordered solid solution phases. It is noted that *all configuration entropies mentioned here are calculated for HEAs assuming they are in the liquid or fully random solid solution state (i.e., using the Boltzmann equation)*:

$$\Delta S_{\text{mix}} = -R \sum_{i=1}^N x_i \ln x_i \quad (2.4)$$

A new parameter,  $\Omega$ , combining effects of  $\Delta S_{\text{mix}}$  and  $\Delta H_{\text{mix}}$  on the stability of multicomponent solid solution, was recently proposed by Yang and Zhang [10, 14, 15]. The parameter  $\Omega$  is defined by

$$\Omega = \frac{T_m \Delta S_{\text{mix}}}{|\Delta H_{\text{mix}}|} \quad (2.5)$$

$$T_m = \sum_{i=1}^N x_i (T_m)_i \quad (2.6)$$

where  $T_m$  is the average melting temperature of the  $N$ -element alloy and  $(T_m)_i$  is the melting point of the  $i$ th component of the alloy. By analyzing the phase formation using the parameters  $\Omega$  and  $\delta$  of various reported multicomponent alloys (shown in Fig. 2.3), new criteria for forming solid solution phases in HEAs were suggested:  $\Omega \geq 1.1$  and  $\delta \leq 6.6\%$ . In contrast, intermetallic compounds and BMGs have larger values of  $\delta$  and smaller values of  $\Omega$ , and the value of  $\Omega$  for BMGs is smaller than that of intermetallic compounds. Figure 2.4 replaces  $\delta$  in Fig. 2.3 by the number of elements,  $N$ . It can be seen that solid solution forming HEAs appear at higher  $\Omega$  and larger  $N$ , while BMGs appear at lower  $\Omega$  and smaller  $N$ .

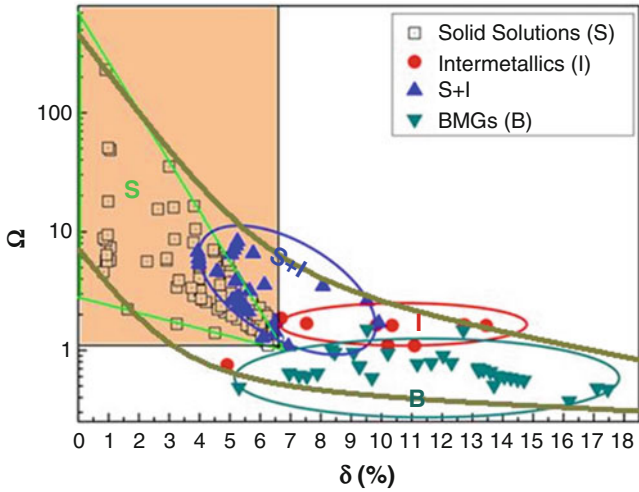


**Fig. 2.3** Phase selection diagram of HEAs and BMGs based on  $\Omega$  and  $\delta$  [16]

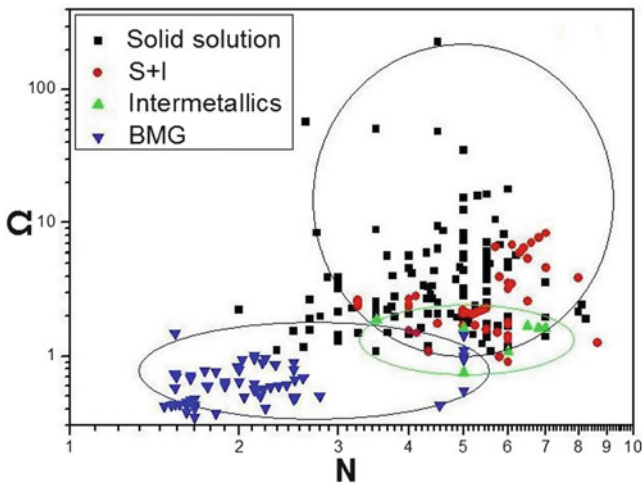


**Fig. 2.4** Phase selection diagram of HEAs and BMGs based on  $\Omega$  and the number of elements,  $N$  [16]

## 2.3 Electron Concentration

HEAs with solid solution structures are generally desired, since most, if not all, advantageous features like high hardness [1], sluggish diffusion kinetics [35], and high-temperature softening resistance [36] are related to the multi-principal-element solid solution structures. The formation of solid solutions in HEAs, as discussed previously, can be reasonably predicted using parametric approaches

based on physiochemical properties of constituent alloying elements, like atomic radii, mixing enthalpies between any two elements, and melting points [7–10]. However, these parametric approaches do not tell much information about the crystal structure of the achieved solid solutions. Since it has been widely known that, based on existing experimental evidences [37], the crystal structure significantly affects the mechanical behavior of HEAs, having the capability to design them with desirable crystal structure is crucial. [The energies of HEAs in fcc, bcc, and hcp structures are presented in Chaps. 7, 8, 9, 10, and 11 using predictive computational methods based on first-principles density functional theory (DFT) and in Chap. 12 using CALPHAD modeling. The  $\Delta H_{\text{mix}}-\delta$  relation is reevaluated based on DFT calculations as presented in Chap. 11.]

The solid solutions formed in HEAs are normally of fcc, bcc, and hcp or a mixture of these structures [37]. fcc-structured HEAs are known to possess good ductility, but with relatively low strength [38]. bcc-structured HEAs can have much higher strength [39], but almost always at the cost of much decreased ductility, particularly in tension. Is it possible to control the formation of fcc- or bcc-structured solid solutions in HEAs? The  $\delta-\Delta H_{\text{mix}}$  plot shown in Fig. 2.5 indicates that the fcc-type solid solutions form at sufficiently small  $\delta$ , and bcc solid solutions form at larger  $\delta$  [16], assuming  $\Delta H_{\text{mix}}$  still satisfies the conditions to form solid solutions. However, the fcc-type solid solution forming  $\delta$  range largely overlaps with that of the bcc solid solutions, which practically means  $\delta$  has limited use in terms of controlling the formation of fcc- or bcc-structured HEAs. As such, new criteria or new parameters need to be established for this important purpose.

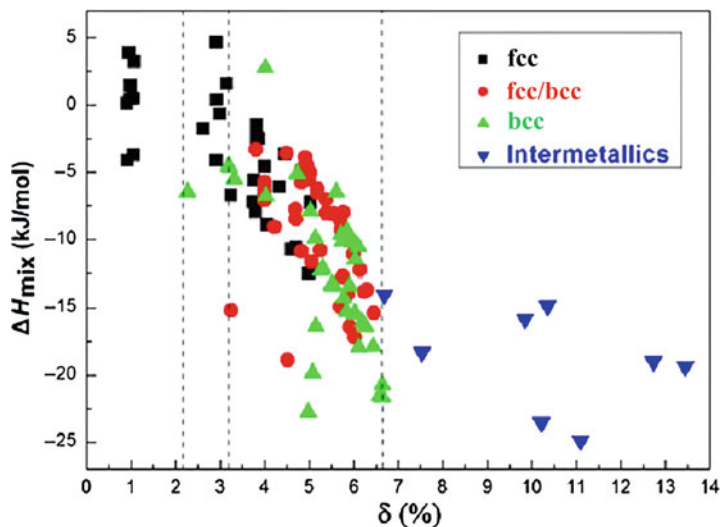


**Fig. 2.5** Dependence of crystal structures on the enthalpy of mixing,  $\Delta H_{\text{mix}}$ , and the atomic size mismatch,  $\delta$ , in various HEAs [16]

Inspirations to address this issue came from the equivalency of alloying elements in stabilizing fcc- or bcc-type solid solutions. It has been widely confirmed by experiments that elements like Al and Cr are bcc phase stabilizers and Ni and Co are fcc phase stabilizers [40]. It was clearly shown that in the  $\text{Al}_x\text{Co}_y\text{Cr}_z\text{Cu}_{0.5}\text{Fe}_v\text{Ni}_w$  alloy system, 1.11 portions of Co was equivalent to 1 portion of Ni as the fcc phase stabilizer, and 2.23 portions of Cr was equivalent to 1 portion of Al as the bcc stabilizer. When the equivalent Co % was greater than 45 at.%, the alloys had an fcc structure; when the equivalent Cr % was greater than 55 at.%, the alloys had a bcc structure [41]. Naturally, this equivalency of alloying elements in stabilizing a particular crystal structure reminds the well-known effect of electron concentration on the crystal structure in conventional alloys [42]. Before the effect of electron concentration on the crystal structure of solid solutions forming HEAs is discussed, two different notions of electron concentrations, valence electron concentration (*VEC*) and electrons per atom ratio (*e/a*), will be introduced first, as there exist subtle differences in their definitions and resulting applications.

### 2.3.1 *VEC and e/a*

Electron concentration has been known to play a critical role in controlling the phase stability and even physical properties of alloys [42]. It is pointed out that two different notions of electron concentration exist, one is the average number of itinerant electrons per atom ratio (*e/a*), and the other is the number of total electrons (*VEC*) (including d electrons involved in the valence band). For example, *e/a* and *VEC* for pure Cu ([Ar] 3d<sup>10</sup>4s<sup>1</sup>) is 1 and 11, respectively. Basically, *e/a* is in connection with the Hume-Rothery electron concentration rule, and *VEC* is a key parameter in first-principles band calculations and is obtained by integrating the density of states (DOS) of the valence band from the bottom up to a given energy. Mizutani discussed different applications of *e/a* and *VEC* in depth in his monograph *Hume-Rothery Rules for Structurally Complex Alloy Phases* [42]. [Interested readers are suggested to refer to this book for more detailed information on the difference between *e/a* and *VEC*.] Some applications of *e/a* and *VEC* in terms of the crystal structure and phase stability are exemplified here, to facilitate the discussions that are followed.

The effect of *e/a* on the phase stability is articulated in the Hume-Rothery rules, where Hume-Rothery noted that similar structures occur at characteristic *e/a* [42]. As a classical example, Fig. 2.6 shows the *e/a* dependence of the phase stability in alloys based on noble metals (Cu-, Ag-, and Au-based alloys) [42]. Seen from Fig. 2.6, the  $\alpha$ -,  $\beta$ -,  $\gamma$ -,  $\epsilon$ -, and  $\eta$ -phases successively appear at particular *e/a* ranges, regardless of the solute element added to noble metals. The fcc  $\alpha$ -phase exists at  $e/a < 1.4$ . Near  $e/a = 1.5$ , the bcc  $\beta$ -phase exists at high temperatures, which is replaced either by its ordered CsCl-type (B2)  $\beta$ -phase or by the hcp  $\zeta$ -phase at low temperatures. Also around  $e/a = 1.5$ , the  $\mu$ -phase containing 20 atoms in its  $\beta$ -Mn-type cubic unit cell occurs in certain alloy systems. The complex cubic

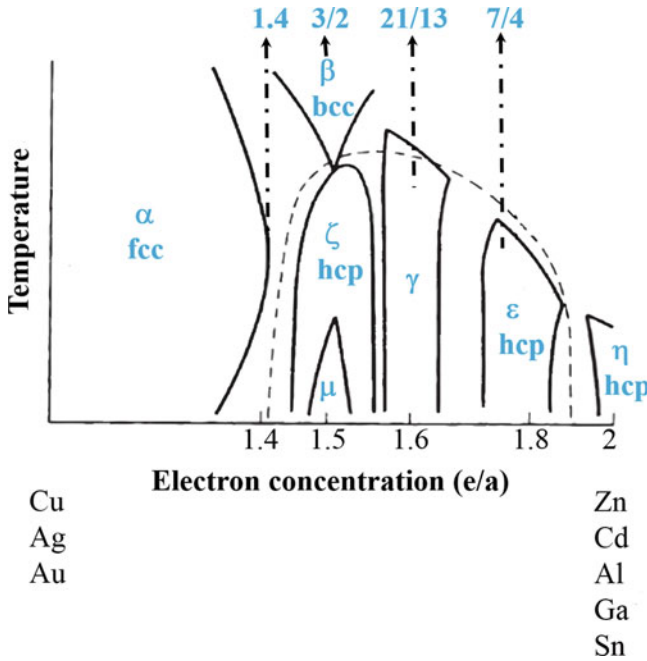


**Fig. 2.6** Schematic phase diagram showing the Hume-Rothery electron concentration ( $e/a$ ) rule in noble metal alloys [42]

$\gamma$ -phase is stabilized at about  $e/a = 1.6$  and the hcp  $\epsilon$ -phase in the range  $1.7 < e/a < 1.9$ . The hcp  $\eta$ -phase appears as a primary solid solution of Zn and Cd and is centered at  $e/a = 2.0$ . This is the Hume-Rothery electron concentration rule. Because of their locations at particular electron concentrations, these alloys are called electron compounds or Hume-Rothery electron phases. Judging from its strong  $e/a$  dependence, it has been naturally thought that the interaction of the Fermi surface with the Brillouin zone must play a critical role in stabilizing these electron phases.

VEC has been proved to be quite effective in controlling the ordered crystal structures of  $\text{Co}_3\text{V}$  alloyed with Fe and Ni [43]. Ni, Co, and Fe have similar atomic sizes and electronegativities, but differ in VEC: 10, 9, and 8, respectively [37]. The stoichiometric  $\text{Co}_3\text{V}$  has a six-layer hexagonal ordered structure with the stacking sequence **ABCACB**. The stacking character of  $\text{Co}_3\text{V}$  is **hcchcc**, with a 33.3 % hexagonality. VEC of  $\text{Co}_3\text{V}$  can be increased by partial replacement of Co by Ni:  $(\text{Ni}, \text{Co})_3\text{V}$ . With increasing VEC, the hexagonality can increase from 33.3 to 100 % at a VEC of 8.54. Further increasing VEC to 8.75, when Ni completely replaces Co, results in a change in the basic layer structure from triangular (T) type to rectangular (R) type, and stacking of the R layers gives a tetragonal ordered structure similar to  $\text{DO}_{22}$ -type  $\text{Ni}_3\text{V}$ . VEC of  $\text{Co}_3\text{V}$  can also be reduced by

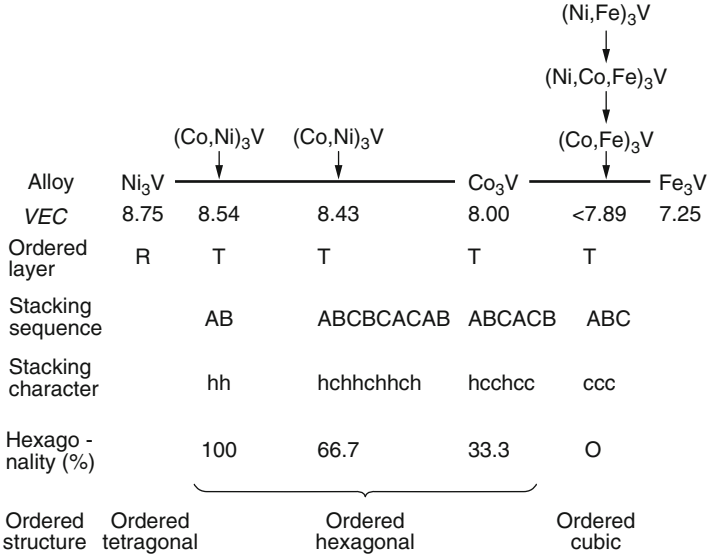


**Fig. 2.7** Effect of the electron concentration ( $VEC$ ) on the stability of ordered crystal structures in  $\text{Ni}_3\text{V}$ - $\text{Co}_3\text{V}$ - $\text{Fe}_3\text{V}$  alloys [43]

partial replacement of Co by Fe:  $(\text{Co}, \text{Fe})_3\text{V}$ . With  $VEC$  below 7.89, the  $L1_2$  ordered cubic structure having the stacking sequence **ABC (ccc)** is stabilized. Controlling the hexagonality of  $\text{Co}_3\text{V}$  alloys by the adjustment of  $VEC$  is very important to the room temperature ductility, as ordered hexagonal alloys are brittle due to the limited number of slip systems, while the deformation behavior of ordered cubic alloys is similar to that of ductile fcc alloys. Indeed, ordered cubic alloys of the compositions of  $(\text{Fe}, \text{Co})_3\text{V}$ ,  $(\text{Fe}, \text{Co}, \text{Ni})_3\text{V}$ , and  $(\text{Fe}, \text{Ni})_3\text{V}$  are all ductile, and ordered hexagonal alloys of the compositions of  $\text{Co}_3\text{V}$  and  $(\text{Ni}, \text{Co})_3\text{V}$  are brittle. The  $VEC$  dependence of the phase stability in  $\text{Co}_3\text{V}$  alloys is shown in Fig. 2.7. Similarly, the  $VEC$  rule has been successfully applied to tune the phase stability (cubic C15 and hexagonal C14 and C36) in  $\text{NbCr}_2$ -based Laves phase alloys [44].

2.3.2  $VEC$  or  $e/a$ ?

As shown above, both  $e/a$  and  $VEC$  have been proved to be correlated to the phase stability and physical properties of alloys. One needs to be cautious in selecting  $e/a$  or  $VEC$  as an electron concentration parameter though, depending on the situation that is involved. Mizutani [42] showed that physical properties, including the saturation magnetization and the electronic specific heat coefficient in 3d transition metals, the superconducting transition temperature of TM (transition metal) alloys,

and the thermoelectric power in the Heusler ( $L2_1$ )-type  $Fe_2VAI$  alloys, all exhibit a universal behavior with respect to  $VEC$ . Mizutani noted that all these properties are clearly related to the total DOS at the Fermi level. Meanwhile, physical properties like the axial ratio,  $c/a$ , the magnetic susceptibility corrected for ionic contributions, and the electronic specific heat coefficient in noble metal alloys are all correlated to  $e/a$ , and not to  $VEC$ . These properties are known to be dominated by the FsBz (Fermi surface-Brillouin zone) interactions and therefore are unsurprisingly scaled in terms of  $e/a$ , which is introduced through the Fermi diameter  $2k_F$  in the matching condition. When discussing the role of two electron concentration parameters  $VEC$  and  $e/a$  in designing new CMAs (complex metallic alloys), which are characterized by a pseudogap across the Fermi level, Mizutani concluded that  $VEC$  can be used as long as a rigid-band model holds, assuming that the electronic density of states of an alloy can be inferred from that of the host, whereas  $e/a$  or  $e/uc$  (electrons per unit cell) is also useful, only if sound  $e/a$  values for the TM elements are used.  $e/a$  values for transition metals have been quite controversial for a long time and no satisfied solutions have yet emerged. This difficulty has challenged the interpretations of the Hume-Rothery electron concentration rule for alloys containing TM elements. Mizutani evaluated different proposals for  $e/a$ , mainly analyzing those postulated by Raynor and by Haworth and Hume-Rothery [42], and then deduced a new set of  $e/a$  values for TM elements based on the Hume-Rothery plot, which is quite different to the previous proposals [42]. The work from Mizutani will not end the discussion on  $e/a$  values for TM elements though, since not all  $e/a$  have been determined, and  $e/a$  for each element even varies depending on the atomic environment. It should be noted that the  $e/a$  rule has also been used to design quasi-crystalline alloys [45, 46] and even amorphous alloys [47, 48], with some success. Nevertheless, the choice of  $e/a$  for TM elements was also ambiguous.

### 2.3.3 The Effect of $VEC$ on the Phase Stability of HEAs

As said previously, the equivalency of alloying elements in stabilizing fcc- or bcc-type solid solutions in HEAs naturally leads one to correlate this equivalency to the electron concentration effect. Since currently developed HEAs comprise mainly TM elements, considering the difficulty of defining the  $e/a$  values for them,  $VEC$  seems to be a more straightforward electron concentration parameter. Meanwhile, it has been shown that in the  $Al_xCo_yCr_zCu_{0.5}Fe_vNi_w$  alloy system, 1.11 portions of Co was equivalent to 1 portion of Ni as the fcc phase stabilizer [41]. This further indicates that  $VEC$  has an effect on the phase stability in HEAs: a  $VEC$  of 9 for Co and 10 for Ni. To verify this, Guo et al. designed a series of  $Al_xCrCuFeNi_2$  alloys [37], fully replacing Co with Ni in the widely studied  $Al_xCoCrCuFeNi$  alloys. It was experimentally proved that the new  $Al_xCrCuFeNi_2$  alloy system showed a very similar trend of phase stability to that of  $Al_xCoCrCuFeNi$  alloys, with the increasing Al concentration. In addition, there seemed to exist threshold  $VEC$  values for forming different types of solid solutions at  $VEC \geq 8.0$ , where sole

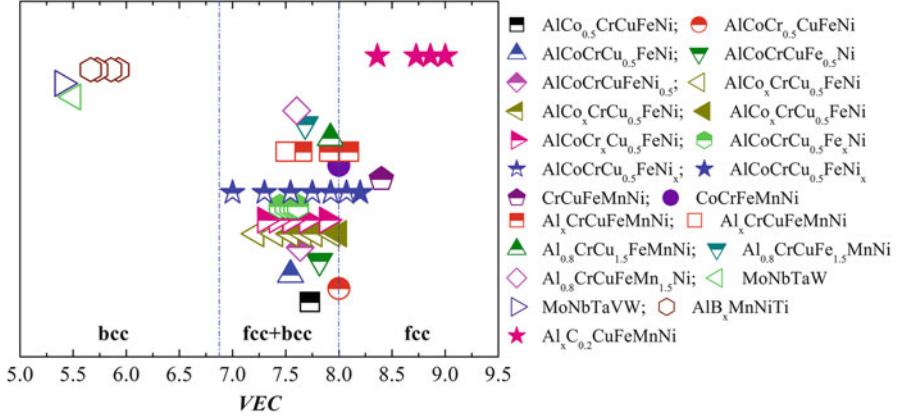


**Fig. 2.8** Relationship between *VEC* and the phase stability for fcc and bcc solid solutions in various HEAs. Note on the legends: fully closed symbols for sole fcc phases, fully open symbols for sole bcc phases, and top-half closed symbols for mixed fcc and bcc phases [37]

fcc solid solution phases formed. Guo et al. then moved to scrutinize the *VEC* effect on the phase stability in various solid solution forming HEAs (where no intermetallic compounds or amorphous phase is formed), comprising different alloying elements. The result of this statistical analysis is shown in Fig. 2.8 [37], from which two important conclusions can be drawn. Firstly and qualitatively, in solid solution forming HEAs, bcc phases are stabilized at a lower *VEC*, while fcc phases are stabilized at a higher *VEC*. In the intermediate *VEC*, both fcc and bcc phases exist. Secondly and almost quantitatively, fcc phases occur at  $VEC \geq 8.0$ , bcc phases at  $VEC < 6.87$ , and a mixture of fcc and bcc phases at  $6.87 \leq VEC < 8$ . Some exceptions do exist, particularly for Mn-containing HEAs. The *VEC* rule provides a convenient way to design fcc- or bcc-structured HEAs containing mainly TM elements, from the electron concentration perspective, and its validity has been verified widely by subsequent experiments following its publication.

A few notes need to be added in terms of utilizing the *VEC* rule. First, the *VEC* rule was proposed based on the experimental results from cast alloys. Its validity to HEAs prepared by other routes (e.g., the powder metallurgy method) has not been evaluated. Second, the *VEC* rule only works on the premise that the solid solutions are the only alloying products (i.e., no intermetallic compounds or amorphous phase is formed). Third, when discussing the separation of fcc and bcc solid solutions, no distinction was made between disordered and ordered solid solutions. For example, B2-type ordered bcc phases and disordered bcc phases were both classified as bcc solid solutions. Fourth, forming the fcc or bcc solid solutions does not necessarily indicate the formation of one fcc or bcc phase. For example, this can mean the formation of two disordered fcc phases or one disordered fcc plus one ordered fcc phase. Fifth, the threshold *VEC* values of 6.87 and 8.0 are mainly for reference. They can vary in different alloy systems [37] and even vary for the same compositions that were cast with different cooling rates [6] or after subsequent heat

treatments at various temperatures [49]. The latter variations are understandable, considering that solid solution phases appearing in cast HEAs are actually frozen stable solid-state phases at elevated temperatures [50] and therefore affected by factors like kinetics and also the entropic contribution to the Gibbs free energy. However, so far there are no exceptions against the trend that a higher *VEC* favors the fcc phase and a lower *VEC* favors the bcc phase, in solid solution forming HEAs. From the published experimental results, the threshold *VEC* values of 6.87 and 8.0 still seem to be a reasonable guidance to design fcc- or bcc-structured HEAs, prepared from the direct casting. Again, it has to be emphasized that, so far this statement has mostly been verified for HEAs containing mainly TM elements.

In the second note that is given above, it is emphasized that the *VEC* rule for the formation of fcc- or bcc-type solid solutions only works when no intermetallic compounds form. In cases when entropic contribution in lowering the Gibbs free energy is not sufficient to surpass the very negative enthalpy among alloying elements, intermetallic compounds form [7]. Interestingly, Tsai et al. showed that *VEC* can also be used to predict the formation of  $\sigma$ -phase in cast Cr- and V-containing HEAs, and furthermore the *VEC* range of the formation of  $\sigma$ -phase was  $6.88 < VEC < 7.84$  (Fig. 2.9). It is interesting to point out that this range almost overlaps with that for forming the mixture of fcc and bcc solid solutions proposed by Guo et al.:  $6.87 \leq VEC < 8$  [51]. No  $\sigma$ -phase was found to form outside this range. Based on these results, it seems probable that the internal energy difference between the mixed fcc and bcc solid solutions and the  $\sigma$ -phase is small. The general applicability of the *VEC* rule to the formation of  $\sigma$ -phase in other alloy systems and to other type of intermetallic compounds is uncertain and still awaits further experimental evidences.

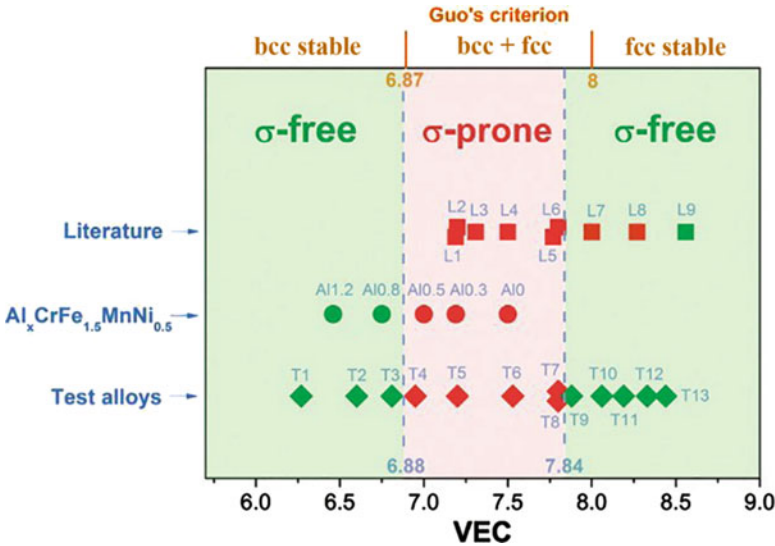


Fig. 2.9 Relationship between *VEC* and the presence of the  $\sigma$ -phase after aging for various HEAs [51]

## 2.4 Remaining Issues and Future Prospects

### 2.4.1 Phase Formation Rules for HEAs Containing Mainly Non-TM Elements

The phase formation rules proposed in Sect. 2.2 are basically based on HEAs containing mainly 3d and/or 4d TM elements. For low-density multicomponent HEAs containing high concentrations of Al, Mg, Li, Zn, Cu, and/or Sn, it was found that most previous phase formation rules fail to work effectively [15]. The configurational entropy seems not to be a dominant factor controlling the phase selection in low-density multicomponent alloys containing significant amounts of Al, Mg, and Li. Compared with HEAs containing mainly TM elements, low-density multicomponent alloys do not readily form solid solution phases with a simple crystal structure. As seen in Fig. 2.10, the threshold values of parametric criteria that are given in Sect. 2.2 need to be modified to be applicable for low-density HEAs containing mainly non-TM elements. Namely, solid solutions form at smaller value of  $\delta$  ( $<4.5\%$ ), larger value of  $\Delta H_{\text{mix}}$  ( $\sim -1 \text{ kJ/mol} < \Delta H_{\text{mix}} \leq 5 \text{ kJ/mol}$ ), and larger value of  $\Omega$  ( $> \sim 10$ ).

### 2.4.2 Justification of the VEC Rule

The validity of the VEC rule in controlling the fcc- or bcc-type solid solution phases in HEAs has been proved by a large amount of experiments. This indicates that the phase stability in HEAs is probably determined by the total DOS at the Fermi level, which can be predicted by first-principles calculations. Widom et al. used first-principles calculations to study the ordering issue in Mo-Nb-Ta-W refractory HEAs [53, 54]. Tian et al. studied the structural stability in CoCrFeNiAl<sub>x</sub> HEAs and they found that at 300 K the fcc phase in these alloys is stable at  $VEC \geq 7.57$  and the bcc phase is stable at  $VEC \leq 7.04$  [55]. These threshold VEC values are not too far away from those proposed by Guo et al. [37]. Firstly, as discussed before, the threshold VEC values proposed by Guo et al. are mainly for reference only and variations among different alloy systems are expected. Secondly, in Tian et al.'s calculation, the relative stability of fcc and bcc phases was compared at 300 K. This would also cause some concerns, as these solid solution phases are not equilibrium phases at room temperature [50]. In order to physically justify the VEC rule, more work from the theoretical side needs to be carried out. For example, temperature may impact the chemical and structural ordering of HEAs to a large degree and consequently their electronic and thermodynamic properties. Furthermore, additional work is required to verify the VEC rule for HEAs not containing mainly TM elements.

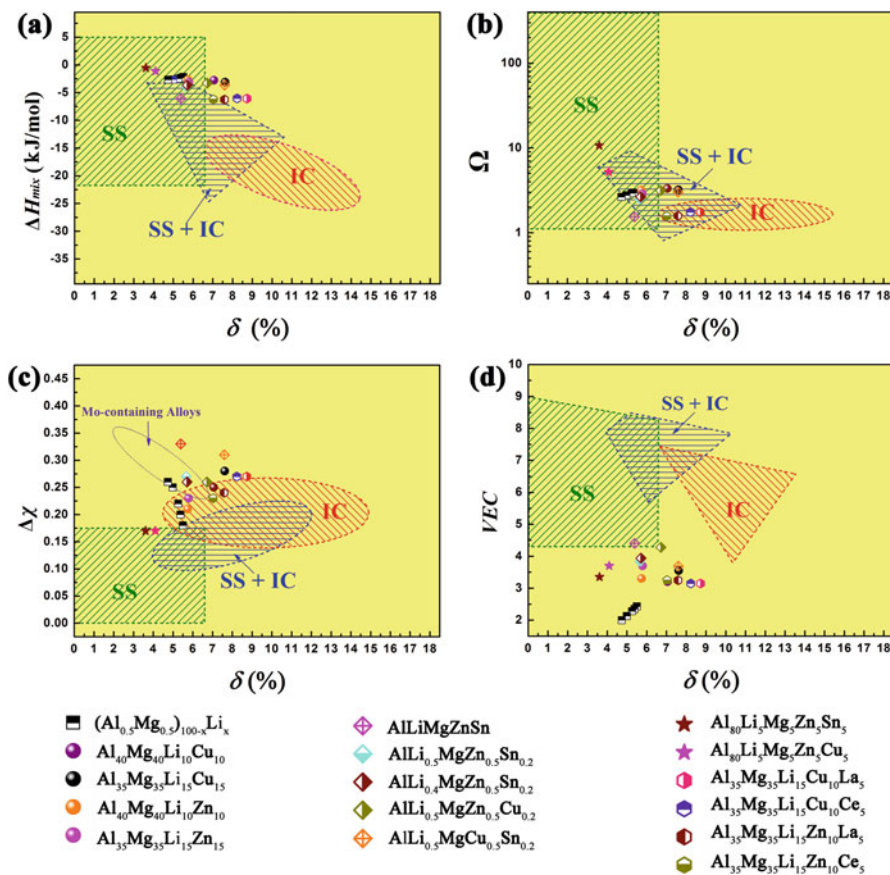


**Fig. 2.10** (a)  $\delta$ - $\Delta H_{\text{mix}}$ , (b)  $\delta$ - $\Omega$ , (c)  $\delta$ - $\Delta\chi$  ( $\Delta\chi$  is the electronegativity difference among elements, defined in Ref. [52]), and (d)  $\delta$ -VEC plots for low-density multicomponent alloys on crosshatched regions developed in previous HEA investigations. For  $(\text{Al}_{0.5}\text{Mg}_{0.5})_{100-x}\text{Li}_x$ ,  $x = 5, 10, 15, 25$ , and  $33.33$  [15]

### 2.4.3 Beyond fcc and bcc Solid Solutions

In almost all available experimental results, if solid solutions are formed in HEAs, these solid solutions are fcc structured, bcc structured, or a mixture of these structures. However, some other types of solid solutions were also found. Recently, Liliensten reported an orthorhombic structure in the  $\text{Ti}_{35}\text{Zr}_{27.5}\text{Hf}_{27.5}\text{Ta}_5\text{Nb}_5$  alloy [56], although whether an alloy of such a composition can be classified as HEAs is debatable. However, hcp-type solid solutions have been experimentally observed or theoretically predicted in high-entropy alloy systems like  $\text{DyGdHoTbY}$ ,  $\text{DyGdLuTbY}$ ,  $\text{DyGbLuTbTm}$ ,  $\text{CoFeMnTi}_x\text{V}_y\text{Zr}_z$ ,  $\text{CrFeNiTiVZr}$ ,  $\text{CoFeNiTi}$ , and

CoOsReRu [57–62]. These alloys pose challenges to the *VEC* rule that was initially established to control the formation of fcc- and bcc-type solid solutions in HEAs. The phase stability dependence on the electron concentration needs to be further understood along with the discovery of new HEAs containing different phase constitutions.

#### 2.4.4 On $e/a$

The difference between *VEC* and  $e/a$ , in terms of both definitions and applications, has been discussed (more details in Ref. [42]). Due to the difficulty in defining the  $e/a$  values for TM elements, the use of *VEC* is more convenient for predicting the phase selection in HEAs. However, based on the historical contribution of  $e/a$  to understand the phase stability in alloys, efforts to study the effect of  $e/a$  on the phase stability in HEAs are still necessary. Poletti and Battezzati recently evaluated the phase stability of HEAs using both  $e/a$  and *VEC* [63]. They claimed that fcc phases are stabilized at  $VEC > 7.5$  and  $1.6 < e/a < 1.8$  and bcc phases are stabilized at  $VEC < 7.5$  and  $1.8 < e/a < 2.3$ . If such a correlation between  $e/a$  and the phase stability does exist, then it provides a new perspective to design HEAs. However, it needs to be noted that when calculating  $e/a$ , they counted the electrons on the  $s$  and  $p$  orbital for all elements, even for TM elements, such as an  $e/a$  of 1 for Cr ([Ar]  $3d^5 4s^1$ ) and 2 for Fe ([Ar]  $3d^6 4s^2$ ) and Ni ([Ar]  $3d^8 4s^2$ ). The choice of  $e/a$ , and hence the soundness of this  $e/a$  dependence of the phase stability, needs more justifications. Nevertheless, it is expected that future work along this line of thinking will help to gain a deeper understanding into the effect of electron concentration on the phase stability of HEAs.

### 2.5 Summary

The phase formation rules in HEAs have been formulated using a parametric approach, utilizing parameters based on two considerations, i.e., thermodynamics and geometry effect. A couple of criteria are proposed to predict and control the phase selection, among solid solutions, intermetallic compounds, and the amorphous phase, in HEAs containing mainly transition metals. These criteria include the enthalpy of mixing,  $\Delta H_{\text{mix}}$ ; the atomic size difference,  $\delta$ ; and the  $\Omega$  parameter. Particularly,  $\Omega \geq 1.1$  and  $\delta \leq 6.6\%$  proved to be quite effective in predicting the solid solutions in HEAs. The formation of intermetallic compounds tends to complicate the phase formation rules, and this still constitutes a challenge to formulate sufficient conditions (i.e., not just necessary conditions) to form solid solutions in HEAs. The applicability of current phase formation rules to HEAs containing mainly non-TM elements needs further inspections.

Inspired by the equivalency of stabilizing elements and also the well-established knowledge on physical metallurgy, the valence electron concentration, *VEC*, has been found to be a good criterion to control the fcc and bcc solid solutions, the two

most common types of solid solutions seen in HEAs. The *VEC* rule enables one to refine the design of HEAs with desired crystal structures, based on the parametric approaches to design solid solution forming HEAs. Essentially, elements with a higher *VEC* tend to stabilize the fcc phase and elements with a lower *VEC* tend to stabilize the bcc phase, and the threshold values of 8.0 and 6.87 can be a quite reasonable guidance. Since the *VEC* rule was proposed, its effectiveness has been verified by a large amount of experiments and awaits further inspections. Its applicability to HEAs prepared by routes other than casting also needs to be evaluated. Theoretical analyses, mainly based on first-principles calculations, are required to elevate the electron concentration dependence of the phase stability in HEAs, from empirical rules to scientific theories. Meanwhile, new developments are necessary to tackle challenges like the formation of solid solutions other than fcc and bcc structures. Another important electron concentration parameter, electrons per atom ratio,  $e/a$ , is worthy of more attention.

**Acknowledgments** Y.Z. and X.Y. would like acknowledge the financial supports from the National Natural Science Foundation of China (NSFC) with grant nos. of 51210105006, 50971019, 50571018, and 51471025 and National High-Tech R&D (863) Program with grant no. of 2009AA03Z113. S.G. thanks the Area of Advance Materials Science from Chalmers University of Technology, for the start-up funding. C.T.L. acknowledges the financial support from the Research Grants Council (RGC) of the Hong Kong government, through the General Research Fund (GRF) with the account number CityU 521411.

## References

1. Yeh JW, Chen SK, Lin SJ, Gan JY, Chin TS, Shun TT, Tsau CH, Chang SY (2004) Nanostructured high-entropy alloys with multiple principal elements: novel alloy design concepts and outcomes. *Adv Eng Mater* 6(5):299–303. doi:[10.1002/adem.200300567](https://doi.org/10.1002/adem.200300567)
2. Otto F, Yang Y, Bei H, George EP (2013) Relative effects of enthalpy and entropy on the phase stability of equiatomic high-entropy alloys. *Acta Mater* 61(7):2628–2638. doi:[10.1016/j.actamat.2013.01.042](https://doi.org/10.1016/j.actamat.2013.01.042)
3. Tong CJ, Chen YL, Chen SK, Yeh JW, Shun TT, Tsau CH, Lin SJ, Chang SY (2005) Microstructure characterization of  $\text{Al}_x\text{CoCrCuFeNi}$  high-entropy alloy system with multiprincipal elements. *Metall Mater Trans A* 36(4):881–893. doi:[10.1007/s11661-005-0283-0](https://doi.org/10.1007/s11661-005-0283-0)
4. Wang WH (2014) High-entropy metallic glasses. *JOM* 10(66):2067–2077. doi:[10.1007/s11837-014-1002-3](https://doi.org/10.1007/s11837-014-1002-3)
5. Miracle DB, Miller JD, Senkov ON, Woodward C, Uchic MD, Tiley J (2014) Exploration and development of high entropy alloys for structural applications. *Entropy* 16(1):494–525. doi:[10.3390/e16010494](https://doi.org/10.3390/e16010494)
6. Singh S, Wanderka N, Murty BS, Glatzel U, Banhart J (2011) Decomposition in multi-component  $\text{AlCoCrCuFeNi}$  high-entropy alloy. *Acta Mater* 59(1):182–190. doi:[10.1016/j.actamat.2010.09.023](https://doi.org/10.1016/j.actamat.2010.09.023)
7. Guo S, Hu Q, Ng C, Liu CT (2013) More than entropy in high-entropy alloys: forming solid solutions or amorphous phase. *Intermetallics* 41:96–103. doi:[10.1016/j.intermet.2013.05.002](https://doi.org/10.1016/j.intermet.2013.05.002)
8. Guo S, Liu CT (2011) Phase stability in high entropy alloys: formation of solid-solution phase or amorphous phase. *Prog Nat Sci:Mater Int* 21(6):433–446. doi:[10.1016/S1002-0071\(12\)60080-X](https://doi.org/10.1016/S1002-0071(12)60080-X)

9. Zhang Y, Zhou YJ, Lin JP, Chen GL, Liaw PK (2008) Solid-solution phase formation rules for multi-component alloys. *Adv Eng Mater* 10(6):534–538. doi:[10.1002/adem.200700240](https://doi.org/10.1002/adem.200700240)
10. Yang X, Zhang Y (2012) Prediction of high-entropy stabilized solid-solution in multi-component alloys. *Mater Chem Phys* 132(2–3):233–238. doi:[10.1016/j.matchemphys.2011.11.021](https://doi.org/10.1016/j.matchemphys.2011.11.021)
11. Cahn RW, Hassen P (1996) *Physical metallurgy*, vol 1, 4th edn. North Holland, Amsterdam
12. Inoue A (2000) Stabilization of metallic supercooled liquid and bulk amorphous alloys. *Acta Mater* 48(1):279–306. [http://dx.doi.org/10.1016/S1359-6454\(99\)00300-6](http://dx.doi.org/10.1016/S1359-6454(99)00300-6)
13. Curtarolo S, Hart GLW, Nardelli MB, Mingo N, Sanvito S, Levy O (2013) The high-throughput highway to computational materials design. *Nat Mater* 12(3):191–201. doi:[10.1038/nmat3568](https://doi.org/10.1038/nmat3568)
14. Zhang Y, Yang X, Liaw PK (2012) Alloy design and properties optimization of high-entropy alloys. *JOM* 64(7):830–838. doi:[10.1007/s11837-012-0366-5](https://doi.org/10.1007/s11837-012-0366-5)
15. Yang X, Chen SY, Cotton JD, Zhang Y (2014) Phase stability of low-density, multiprincipal component alloys containing aluminum, magnesium, and lithium. *JOM* 10(66):2009–2020. doi:[10.1007/s11837-014-1059-z](https://doi.org/10.1007/s11837-014-1059-z)
16. Zhang Y, Lu ZP, Ma SG, Liaw PK, Tang Z, Cheng YQ, Gao MC (2014) Guidelines in predicting phase formation of high-entropy alloys. *MRS Commun* 4(2):57–62. doi:[10.1557/mrc.2014.11](https://doi.org/10.1557/mrc.2014.11)
17. Ma SG, Zhang Y (2012) Effect of Nb addition on the microstructure and properties of AlCoCrFeNi high-entropy alloy. *Mater Sci Eng A* 532:480–486. doi:[10.1016/j.msea.2011.10.110](https://doi.org/10.1016/j.msea.2011.10.110)
18. Zhang KB, Fu ZY (2012) Effects of annealing treatment on phase composition and microstructure of CoCrFeNiTiAl<sub>x</sub> high-entropy alloys. *Intermetallics* 22:24–32. doi:[10.1016/j.intermet.2011.10.010](https://doi.org/10.1016/j.intermet.2011.10.010)
19. Chuang MH, Tsai MH, Wang WR, Lin SJ, Yeh JW (2011) Microstructure and wear behavior of Al<sub>x</sub>Co<sub>1.5</sub>CrFeNi<sub>1.5</sub>Ti<sub>y</sub> high-entropy alloys. *Acta Mater* 59(16):6308–6317. doi:[10.1016/j.actamat.2011.06.041](https://doi.org/10.1016/j.actamat.2011.06.041)
20. Lucas MS, Mauger L, Munoz JA, Xiao YM, Sheets AO, Semiatin SL, Horwath J, Turgut Z (2011) Magnetic and vibrational properties of high-entropy alloys. *J Appl Phys* 109(7):07E307. doi:[10.1063/1.3538936](https://doi.org/10.1063/1.3538936)
21. Senkov ON, Scott JM, Senkova SV, Miracle DB, Woodward CF (2011) Microstructure and room temperature properties of a high-entropy TaNbHfZrTi alloy. *J Alloys Compd* 509(20):6043–6048. doi:[10.1016/j.jallcom.2011.02.171](https://doi.org/10.1016/j.jallcom.2011.02.171)
22. Zhu JM, Fu HM, Zhang HF, Wang AM, Li H, Hu ZQ (2010) Synthesis and properties of multiprincipal component AlCoCrFeNiSi<sub>x</sub> alloys. *Mater Sci Eng A* 527(27–28):7210–7214. doi:[10.1016/j.msea.2010.07.049](https://doi.org/10.1016/j.msea.2010.07.049)
23. Zhu JM, Fu HM, Zhang HF, Wang AM, Li H, Hu ZQ (2010) Microstructures and compressive properties of multicomponent AlCoCrFeNiMo<sub>x</sub> alloys. *Mater Sci Eng A* 527(26):6975–6979. doi:[10.1016/j.msea.2010.07.028](https://doi.org/10.1016/j.msea.2010.07.028)
24. Hsu CY, Juan CC, Wang WR, Sheu TS, Yeh JW, Chen SK (2011) On the superior hot hardness and softening resistance of AlCoCr<sub>x</sub>FeMo<sub>0.5</sub>Ni high-entropy alloys. *Mater Sci Eng A* 528(10–11):3581–3588. doi:[10.1016/j.msea.2011.01.072](https://doi.org/10.1016/j.msea.2011.01.072)
25. Gao XQ, Zhao K, Ke HB, Ding DW, Wang WH, Bai HY (2011) High mixing entropy bulk metallic glasses. *J Non Cryst Solids* 357(21):3557–3560. doi:[10.1016/j.jnoncrysol.2011.07.016](https://doi.org/10.1016/j.jnoncrysol.2011.07.016)
26. Zhang B, Wang RJ, Zhao DQ, Pan MX, Wang WH (2004) Properties of Ce-based bulk metallic glass-forming alloys. *Phys Rev B* 70(22):224208. doi:[10.1103/PhysRevB.70.224208](https://doi.org/10.1103/PhysRevB.70.224208)
27. Xu DH, Duan G, Johnson WL, Garland C (2004) Formation and properties of new Ni-based amorphous alloys with critical casting thickness up to 5 mm. *Acta Mater* 52(12):3493–3497. doi:[10.1016/j.actamat.2004.04.001](https://doi.org/10.1016/j.actamat.2004.04.001)
28. Jiang QK, Zhang GQ, Chen LY, Wu JZ, Zhang HG, Jiang JZ (2006) Glass formability, thermal stability and mechanical properties of La-based bulk metallic glasses. *J Alloys Compd* 424(1–2):183–186. doi:[10.1016/j.jallcom.2006.07.109](https://doi.org/10.1016/j.jallcom.2006.07.109)

29. Jiang QK, Zhang GQ, Yang L, Wang XD, Saksl K, Franz H, Wunderlich R, Fecht H, Jiang JZ (2007) La-based bulk metallic glasses with critical diameter up to 30 mm. *Acta Mater* 55 (13):4409–4418. doi:[10.1016/j.actamat.2007.04.021](https://doi.org/10.1016/j.actamat.2007.04.021)
30. Chang CT, Shen BL, Inoue A (2006) Co-Fe-B-Si-Nb bulk glassy alloys with superhigh strength and extremely low magnetostriction. *Appl Phys Lett* 88(1):011901. doi:[10.1063/1.2159107](https://doi.org/10.1063/1.2159107)
31. Zhang T, Yang Q, Ji YF, Li R, Pang SJ, Wang JF, Xu T (2011) Centimeter-scale-diameter Co-based bulk metallic glasses with fracture strength exceeding 5000 MPa. *Chin Sci Bull* 56 (36):3972–3977. doi:[10.1007/s11434-011-4765-8](https://doi.org/10.1007/s11434-011-4765-8)
32. Li S, Xi XK, Wei YX, Luo Q, Wang YT, Tang MB, Zhang B, Zhao ZF, Wang RJ, Pan MX, Zhao DQ, Wang WH (2005) Formation and properties of new heavy rare-earth-based bulk metallic glasses. *Sci Techno Adv Mater* 6(7):823–827. doi:[10.1016/j.stam.2005.06.019](https://doi.org/10.1016/j.stam.2005.06.019)
33. Jiang QK, Zhang GQ, Chen LY, Zeng QS, Jiang JZ (2006) Centimeter-sized ( $\text{La}_{0.5}\text{Ce}_{0.5}$ )-based bulk metallic glasses. *J Alloys Compd* 424(1–2):179–182. doi:[10.1016/j.jallcom.2006.07.007](https://doi.org/10.1016/j.jallcom.2006.07.007)
34. Li R, Pang SJ, Men H, Ma CL, Zhang T (2006) Formation and mechanical properties of (Ce-La-Pr-Nd)-Co-Al bulk glassy alloys with superior glass-forming ability. *Scr Mater* 54 (6):1123–1126. doi:[10.1016/j.scriptamat.2005.11.074](https://doi.org/10.1016/j.scriptamat.2005.11.074)
35. Tsai KY, Tsai MH, Yeh JW (2013) Sluggish diffusion in Co-Cr-Fe-Mn-Ni high-entropy alloys. *Acta Mater* 61(13):4887–4897. doi:[10.1016/j.actamat.2013.04.058](https://doi.org/10.1016/j.actamat.2013.04.058)
36. Wu WH, Yang CC, Yeh JW (2006) Industrial development of high-entropy alloys. *Ann Chimie Sci Materiaux* 31(6):737–747. doi:[10.3166/acsm.31.737-747](https://doi.org/10.3166/acsm.31.737-747)
37. Guo S, Ng C, Lu J, Liu CT (2011) Effect of valence electron concentration on stability of fcc or bcc phase in high entropy alloys. *J Appl Phys* 109(10):103505. doi:[10.1063/1.3587228](https://doi.org/10.1063/1.3587228)
38. Wang FJ, Zhang Y, Chen GL, Davies HA (2009) Tensile and compressive mechanical behavior of a  $\text{CoCrCuFeNiAl}_{0.5}$  high entropy alloy. *Int J Mod Phys B* 23(6–7):1254–1259. doi:[10.1142/S0217979209060774](https://doi.org/10.1142/S0217979209060774)
39. Senkov ON, Wilks GB, Miracle DB, Chuang CP, Liaw PK (2010) Refractory high-entropy alloys. *Intermetallics* 18(9):1758–1765. doi:[10.1016/j.intermet.2010.05.014](https://doi.org/10.1016/j.intermet.2010.05.014)
40. Tung CC, Yeh JW, Shun TT, Chen SK, Huang YS, Chen HC (2007) On the elemental effect of  $\text{AlCoCrCuFeNi}$  high-entropy alloy system. *Mater Lett* 61(1):1–5. doi:[10.1016/j.matlet.2006.03.140](https://doi.org/10.1016/j.matlet.2006.03.140)
41. Ke GY, Chen SK, Hsu T, Yeh JW (2006) FCC and BCC equivalents in as-cast solid solutions of  $\text{Al}_x\text{Co}_y\text{Cr}_z\text{Cu}_{0.5}\text{Fe}_v\text{Ni}_w$  high-entropy alloys. *Ann Chimie Sci Materiaux* 31(6):669–683. doi:[10.3166/acsm.31.669-684](https://doi.org/10.3166/acsm.31.669-684)
42. Mizutani U (2011) Hume-Rothery rules for structurally complex alloy phases. CRC Press, Boca Raton
43. Liu CT, Stiegler JO (1984) Ductile ordered intermetallic alloys. *Science* 226(4675):636–642. doi:[10.1126/science.226.4675.636](https://doi.org/10.1126/science.226.4675.636)
44. Zhu JH, Liaw PK, Liu CT (1997) Effect of electron concentration on the phase stability of  $\text{NbCr}_2$ -based Laves phase alloys. *Mater Sci Eng A* 239–240:260–264. doi:[10.1016/S0921-5093\(97\)00590-X](https://doi.org/10.1016/S0921-5093(97)00590-X)
45. Tsai AP, Inoue A, Yokoyama Y, Masumoto T (1990) Stable icosahedral Al-Pd-Mn and Al-Pd-Re alloys. *Mater Trans JIM* 31(2):98–103. doi:[10.2320/matertrans1989.31.98](https://doi.org/10.2320/matertrans1989.31.98)
46. Yokoyama Y, Tsai AP, Inoue A, Masumoto T, Chen HS (1991) Formation criteria and growth-morphology of quasi-crystals in Al-Pd-TM (TM = transition metal) alloys. *Mater Trans JIM* 32(5):421–428. doi:[10.2320/matertrans1989.32.421](https://doi.org/10.2320/matertrans1989.32.421)
47. Chen W, Wang Y, Qiang J, Dong C (2003) Bulk metallic glasses in the Zr-Al-Ni-Cu system. *Acta Mater* 51(7):1899–1907. doi:[10.1016/s1359-6454\(02\)00596-7](https://doi.org/10.1016/s1359-6454(02)00596-7)
48. Dong C, Wang Q, Qiang JB, Wang YM, Jiang N, Han G, Li YH, Wu J, Xia JH (2007) From clusters to phase diagrams: composition rules of quasicrystals and bulk metallic glasses. *J Phys D Appl Phys* 40(15):R273–R291. doi:[10.1088/0022-3727/40/15/r01](https://doi.org/10.1088/0022-3727/40/15/r01)

49. Wang Z, Guo S, Liu CT (2014) Phase selection in high-entropy alloys: From nonequilibrium to equilibrium. *JOM* 10(66):1966–1972. doi:[10.1007/s11837-014-0953-8](https://doi.org/10.1007/s11837-014-0953-8)
50. Ng C, Guo S, Luan JH, Shi SQ, Liu CT (2012) Entropy-driven phase stability and slow diffusion kinetics in  $\text{Al}_{0.5}\text{CoCrCuFeNi}$  high entropy alloy. *Intermetallics* 31:165–172. doi:[10.1016/j.intermet.2012.07.001](https://doi.org/10.1016/j.intermet.2012.07.001)
51. Tsai MH, Tsai KY, Tsai CW, Lee C, Juan CC, Yeh JW (2013) Criterion for sigma phase formation in Cr- and V-containing high-entropy alloys. *Mater Res Lett* 1(4):207–212. doi:[10.1080/21663831.2013.831382](https://doi.org/10.1080/21663831.2013.831382)
52. Fang SS, Xiao X, Lei X, Li WH, Dong YD (2003) Relationship between the widths of supercooled liquid regions and bond parameters of Mg-based bulk metallic glasses. *J Non Cryst Solids* 321(1–2):120–125. doi:[10.1016/s0022-3093\(03\)00155-8](https://doi.org/10.1016/s0022-3093(03)00155-8)
53. Widom M, Huhn WP, Maiti S, Steurer W (2014) Hybrid Monte Carlo/molecular dynamics simulation of a refractory metal high entropy alloy. *Metall Mater Trans A* 45(1):196–200. doi:[10.1007/s11661-013-2000-8](https://doi.org/10.1007/s11661-013-2000-8)
54. Huhn WP, Widom M (2013) Prediction of A2 to B2 phase transition in the high-entropy alloy Mo-Nb-Ta-W. *JOM* 65(12):1772–1779. doi:[10.1007/s11837-013-0772-3](https://doi.org/10.1007/s11837-013-0772-3)
55. Tian FY, Delczeg L, Chen NX, Varga LK, Shen J, Vitos L (2013) Structural stability of  $\text{NiCoFeCrAl}_x$  high-entropy alloy from ab initio theory. *Phys Rev B* 88(8):085128. doi:[10.1103/PhysRevB.88.085128](https://doi.org/10.1103/PhysRevB.88.085128)
56. Lilensten L, Couzinié JP, Perrière L, Bourgon J, Emery N, Guillot I (2014) New structure in refractory high-entropy alloys. *Mater Lett* 132:123–125. doi:[10.1016/j.matlet.2014.06.064](https://doi.org/10.1016/j.matlet.2014.06.064)
57. Kao YF, Chen SK, Sheu JH, Lin JT, Lin WE, Yeh JW, Lin SJ, Liou TH, Wang CW (2010) Hydrogen storage properties of multi-principal-component  $\text{CoFeMnTi}_x\text{V}_y\text{Zr}_z$  alloys. *Int J Hydrogen Energy* 35(17):9046–9059. doi:[10.1016/j.ijhydene.2010.06.012](https://doi.org/10.1016/j.ijhydene.2010.06.012)
58. Kuncce I, Polanski M, Bystrzycki J (2013) Structure and hydrogen storage properties of a high entropy  $\text{ZrTiVCrFeNi}$  alloy synthesized using Laser Engineered Net Shaping (LENS). *Int J Hydrogen Energy* 38(27):12180–12189. doi:[10.1016/j.ijhydene.2013.05.071](https://doi.org/10.1016/j.ijhydene.2013.05.071)
59. Tsau C-H (2009) Phase transformation and mechanical behavior of  $\text{TiFeCoNi}$  alloy during annealing. *Mater Sci Eng A* 501(1–2):81–86. doi:[10.1016/j.msea.2008.09.046](https://doi.org/10.1016/j.msea.2008.09.046)
60. Gao MC, Alman DE (2013) Searching for Next Single-Phase high-entropy alloy compositions. *Entropy* 15(10):4504–4519. doi:[10.3390/e15104504](https://doi.org/10.3390/e15104504)
61. Takeuchi A, Amiya K, Wada T, Yubuta K, Zhang W (2014) High-entropy alloys with a hexagonal close-packed structure designed by equi-atomic alloy strategy and binary phase diagrams. *JOM* 10(66):1984–1992. doi:[10.1007/s11837-014-1085-x](https://doi.org/10.1007/s11837-014-1085-x)
62. Feuerbacher M, Heidelmann M, Thomas C (2014) Hexagonal high-entropy alloys. *Mater Res Lett* 3:1–6. doi:[10.1080/21663831.2014.951493](https://doi.org/10.1080/21663831.2014.951493)
63. Poletti MG, Battezzati L (2014) Electronic and thermodynamic criteria for the occurrence of high entropy alloys in metallic systems. *Acta Mater* 75:297–306. doi:[10.1016/j.actamat.2014.04.033](https://doi.org/10.1016/j.actamat.2014.04.033)

High-Entropy Alloys

Fundamentals and Applications

Gao, M.C.; Yeh, J.-W.; Liaw, P.K.; Zhang, Y. (Eds.)

2016, XIII, 516 p. 233 illus., 187 illus. in color.,

Hardcover

ISBN: 978-3-319-27011-1